Phase coherent transport in hybrid superconductor-topological insulator devices

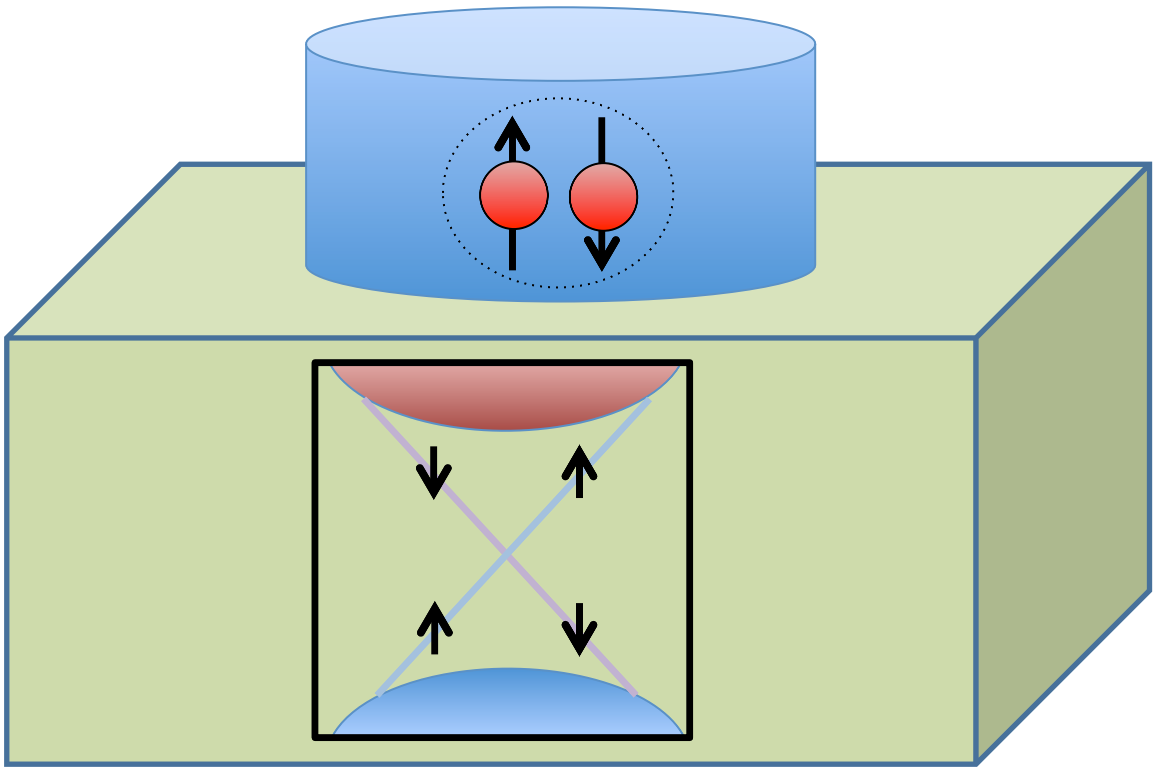

A.D.K. Finck, C. Kurter, P. Ghaemi,
Y.S. Hor, D.J. Van Harlingen

Univ. of Illinois

FS-MRL and Microsoft

Outline

I. **<u>Background</u>**: Majorana Fermions and Topological Insulators.

II. **<u>Fabry-Perot Interference</u>**

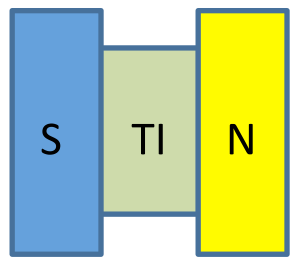

III. **<u>Aharonov-Bohm Interferometry</u>**

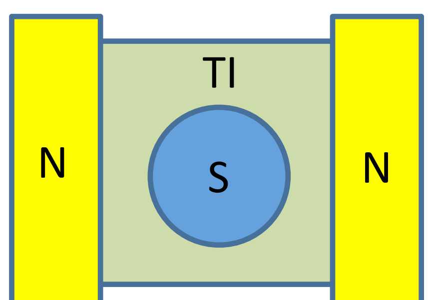

Majorana Fermions

- Majorana equation $\boxed{i\not{\partial}\psi = m\psi_c}$

Ettore Majorana, 1937

- particle = antiparticle $\gamma = \gamma^{+}$

$$\gamma_1 = \tfrac{1}{2}(c^{+} + c)$$

$$\gamma_2 = \tfrac{i}{2}(c^{+} - c)$$

$$\longrightarrow \quad c = \gamma_1 + i\gamma_2$$

- Particle-hole symmetry

$\gamma_{\varepsilon} = \gamma_{-\varepsilon}^{+}$ If ε=0 $\gamma_0 = \gamma_0^{+}$ Majorana !

Vortices in Superconductors

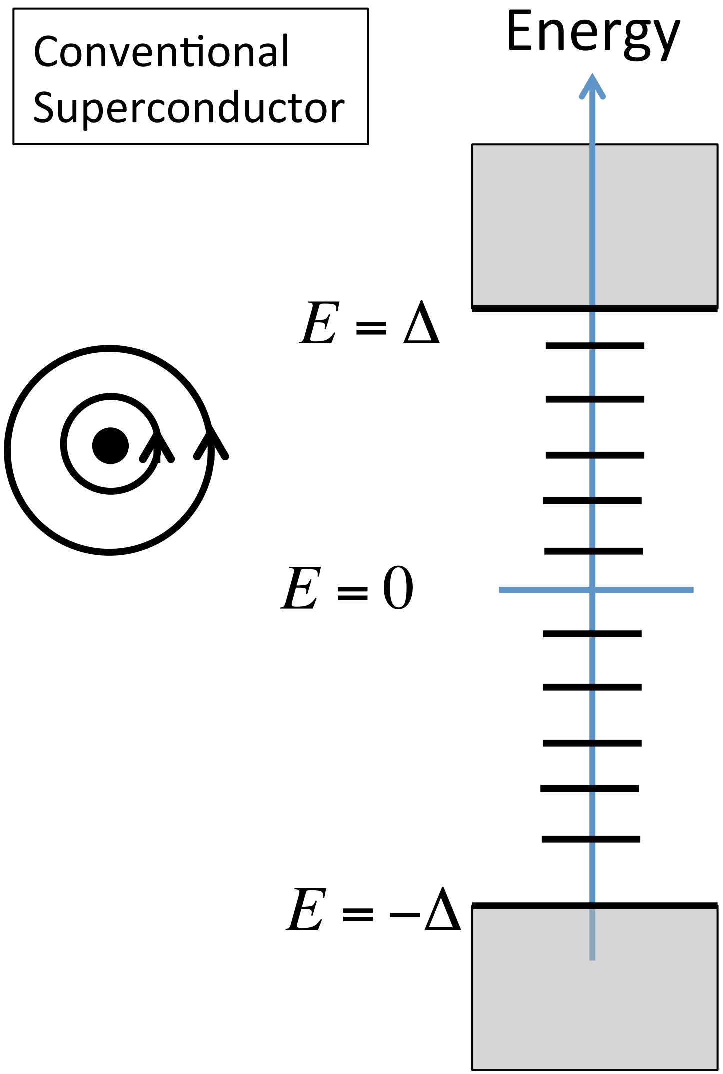

Caroli et al, Phys Lett **9**, 307 (1964)

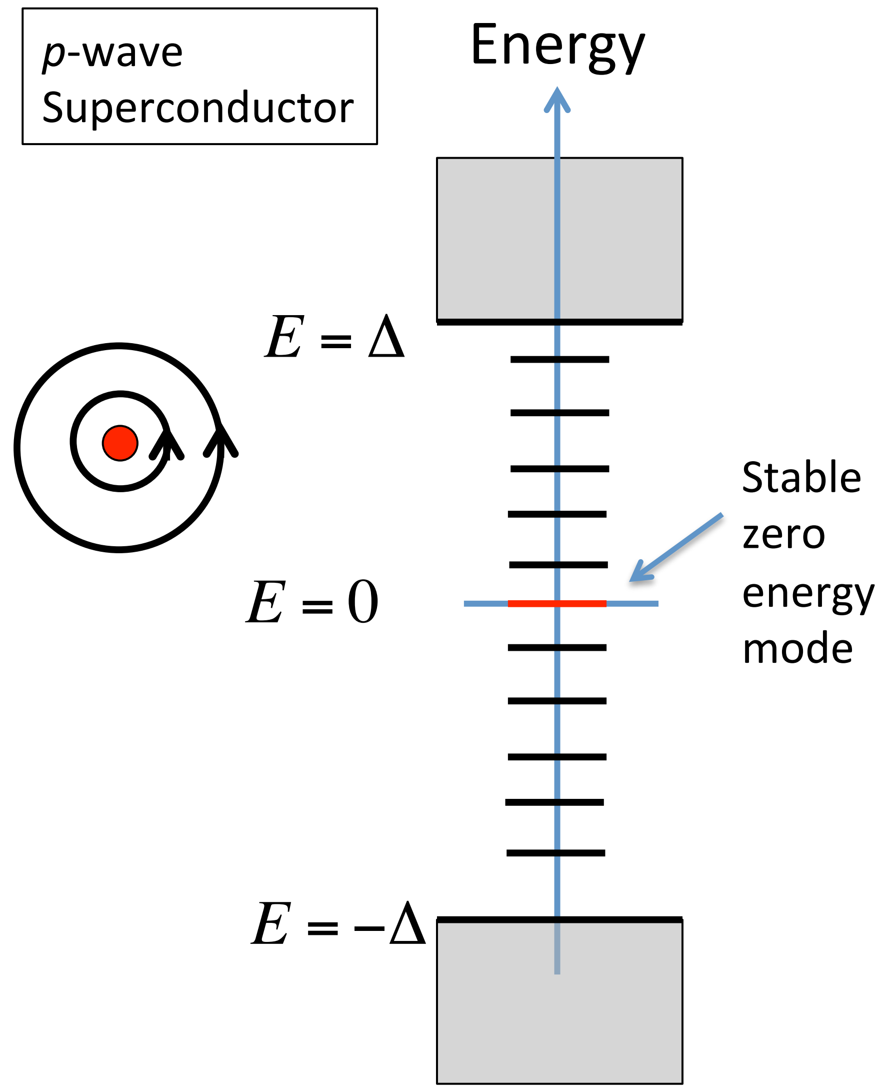

Read and Green, Phys Rev B **61**, 10267 (2000)

Braiding Majoranas

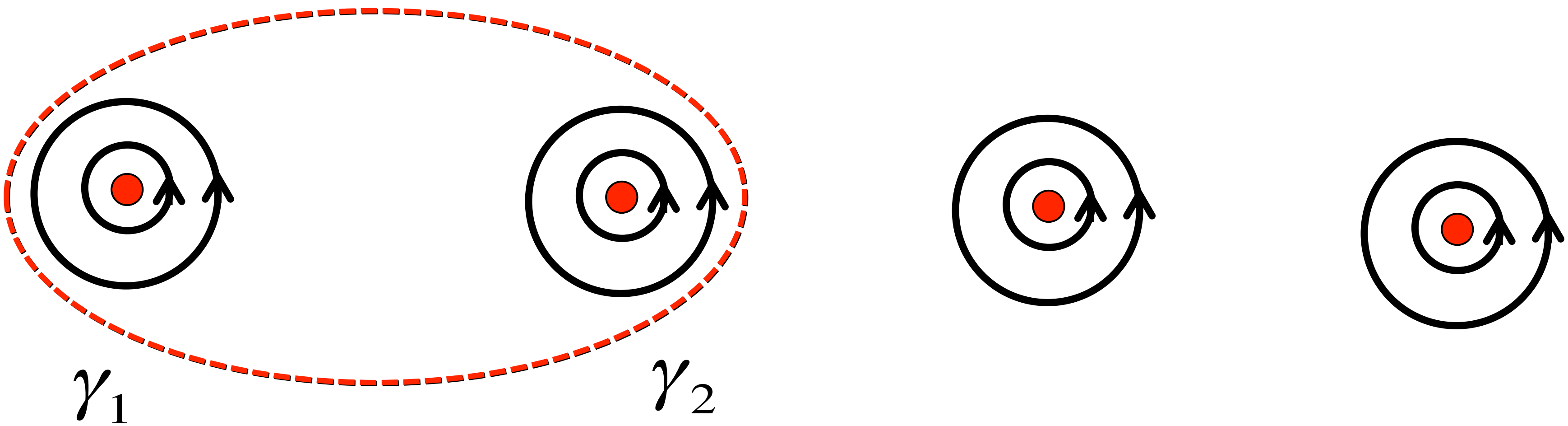

$$c = \gamma_1 + i\gamma_2$$

C. Nayak et al., Rev. Mod. Phys **80**, 1083 (2008).

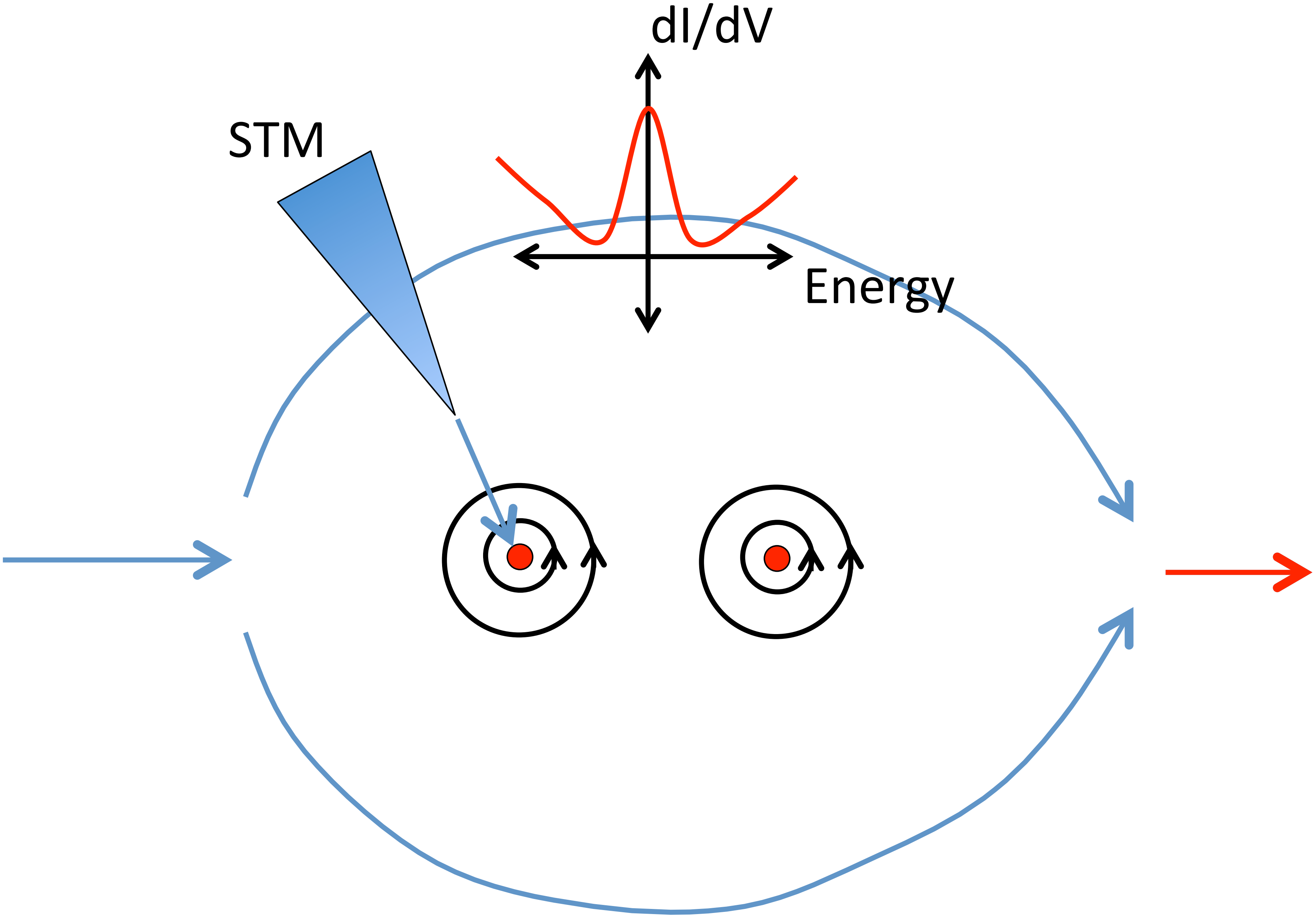

dI/dV
STM
Energy

Realizations of p-wave Superconductor

- "Naturally" occuring
  - Strontium ruthenate (Sr_2RuO_4)
- Fractional Quantum Hall systems
  - 5/2
- Semiconductors with spin-orbit coupling and superconductivity
  - InAs/InSb nanowires in high fields
  - HgTe or InAs/GaSb quantum wells
  - **3D Topological insulators: Bi_2Se_3 or Bi_2Te_3**

3D Topological Insulators

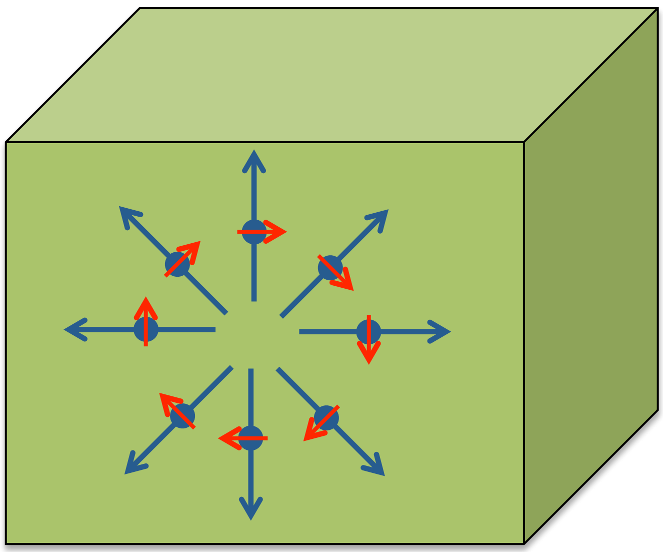

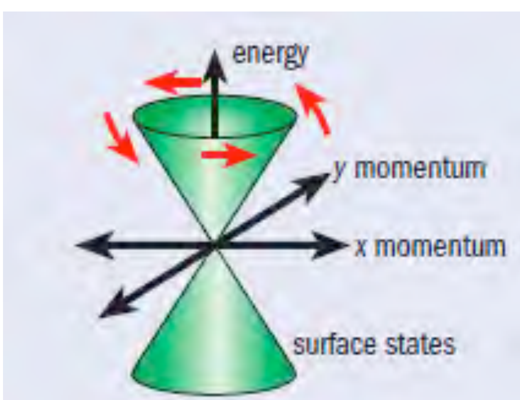

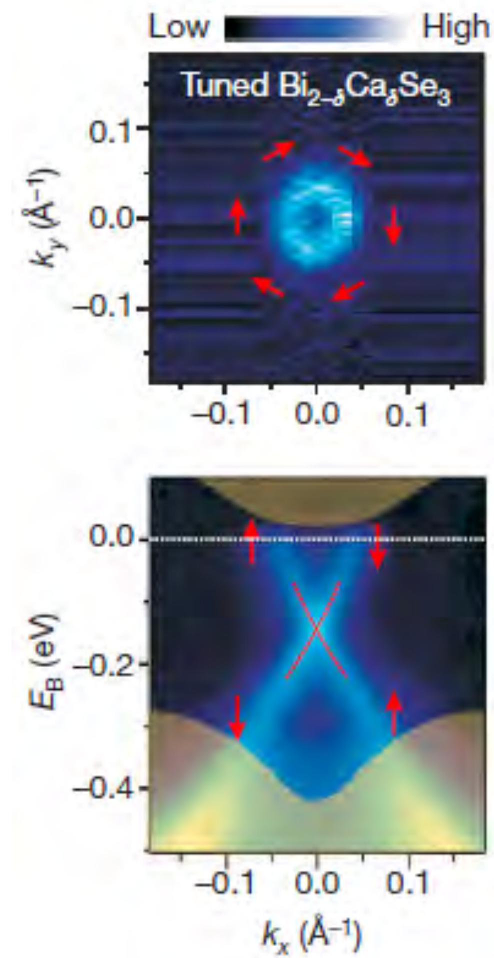

Adapted from Kane and Moore, Physics World 2011.

Hsieh et al., Nature 2009.

Topological Insulator with Superconductivity

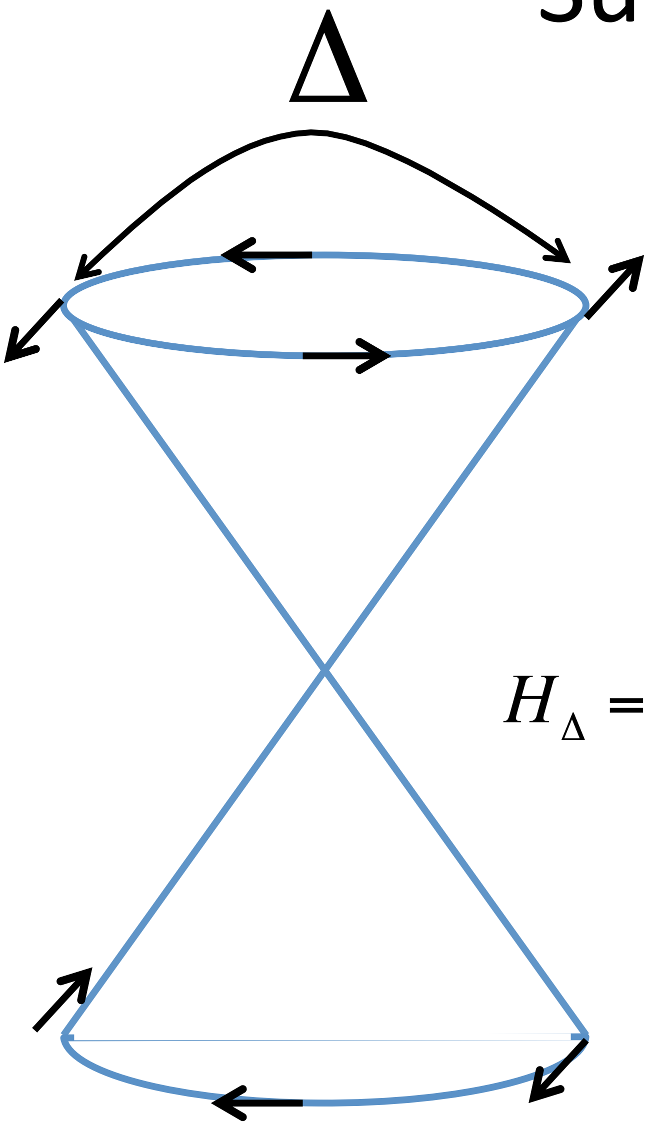

Use helicity basis:

$$\psi_{\pm}(\vec{k}) = \frac{1}{\sqrt{2}}(\psi_{\uparrow}(\vec{k}) \pm e^{i\theta_k}\psi_{\downarrow}(\vec{k}))$$

$$\vec{k} = k_0(\cos\theta_k, \sin\theta_k)$$

$$H_{\Delta} = \sum_{s=\pm}\int \frac{d^2\vec{k}}{(2\pi)^2}\left[\frac{\Delta}{2}\left(\frac{k_x + ik_y}{\left|\vec{k}\right|}\right)\psi_s(\vec{k})\psi_s(\vec{k}) + H.c.\right]$$

Spinless p_x+ip_y pairing due to 2π winding of electron spin.

L. Fu, C. Kane, Phys. Rev. Lett. 100, 096407 (2008)

Inducing Superconductivity via Andreev Reflection

Niobium:

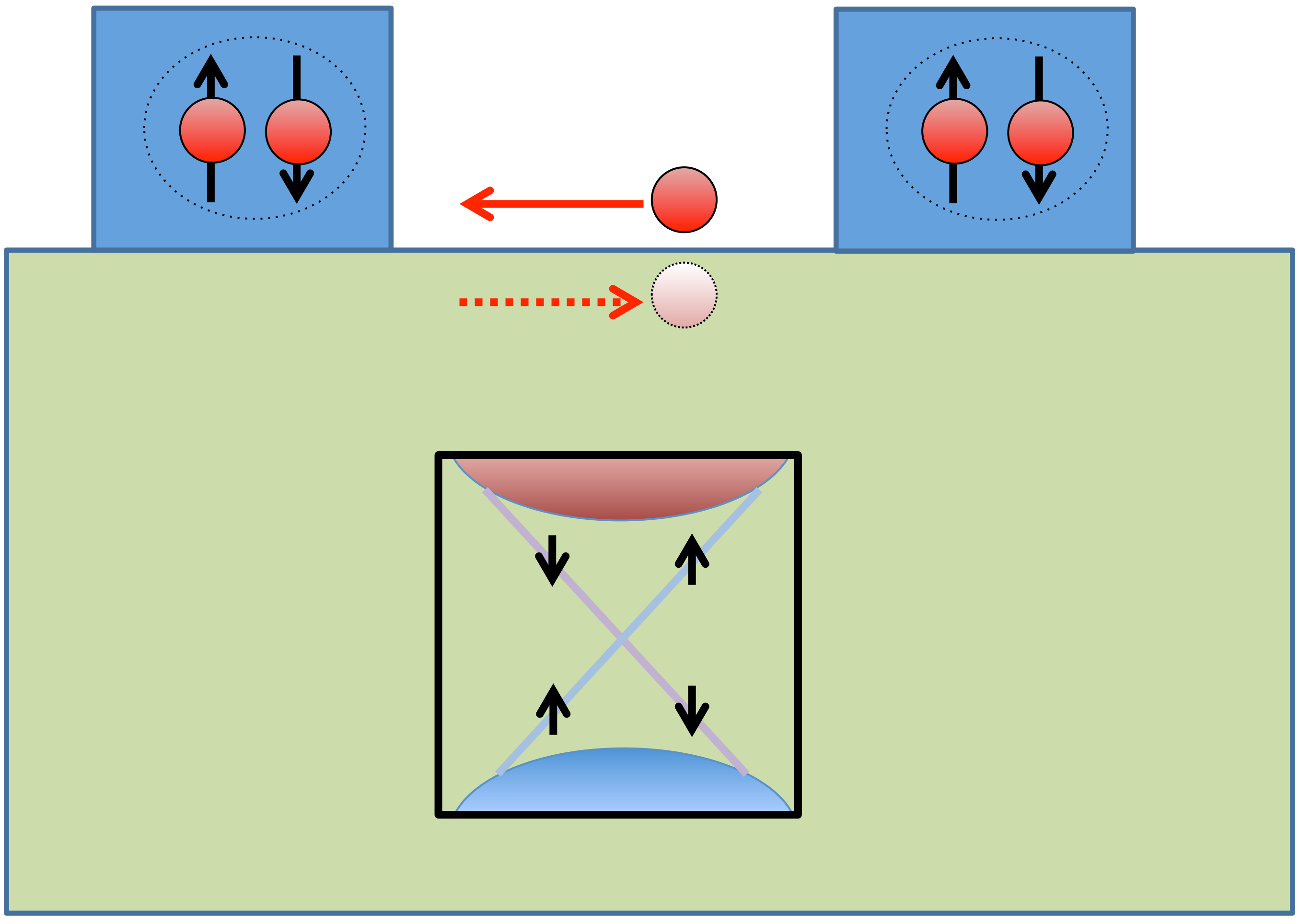

Bi_2Se_3:

Majorana Fermions in Topological Insulators with Superconductivity

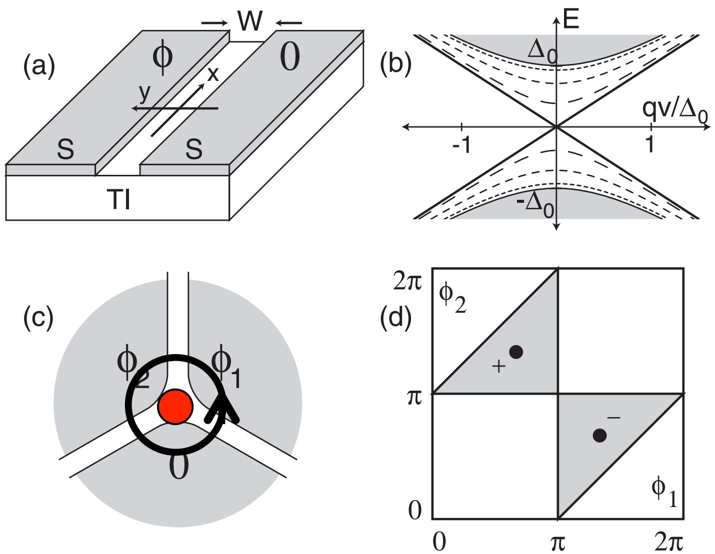

FIG. 1. (a) A STIS line junction. (b) Spectrum of a line junction for $W = \mu = 0$ as a function of momentum for various ϕ. The solid line shows the Andreev bound states for $\phi = \pi$. The dashed lines are for $\phi = 3\pi/4$, $\pi/2$, and $\pi/4$. The bound states for $\phi = 0$ merge with the continuum, indicated by the shaded region. (c) A trijunction between three superconductors. (d) Phase diagram for the trijunction. In the shaded regions there is a $\pm$ MBS at the junction.

Spectrum of Andreev bound states:

$$E_{\pm} = \pm\sqrt{v^2 q^2 + \Delta_0^2 \cos^2(\tfrac{\phi}{2})}$$

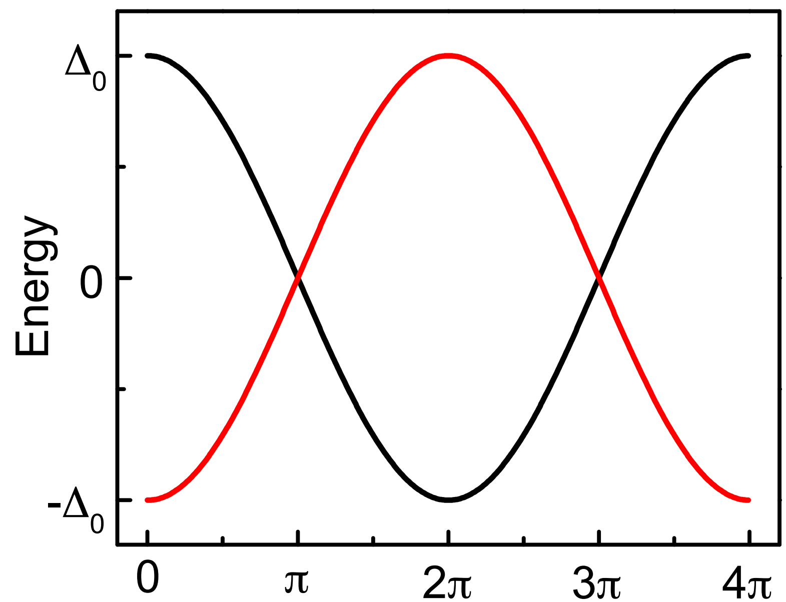

L. Fu, C. Kane, Phys. Rev. Lett. 100, 096407 (2008)

Experimental Techniques

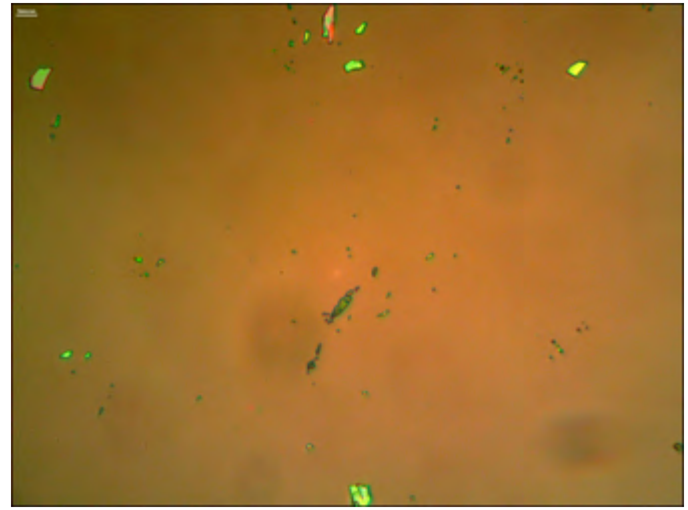

Typical material parameters:

Mobility: 100-1000 cm^2 / V-s
Carrier density: 1e13 – 1e14 cm^{-2}
Coherence length: ~1 micron

Josephson Effect in TI

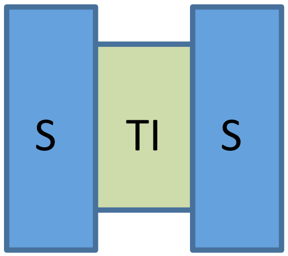

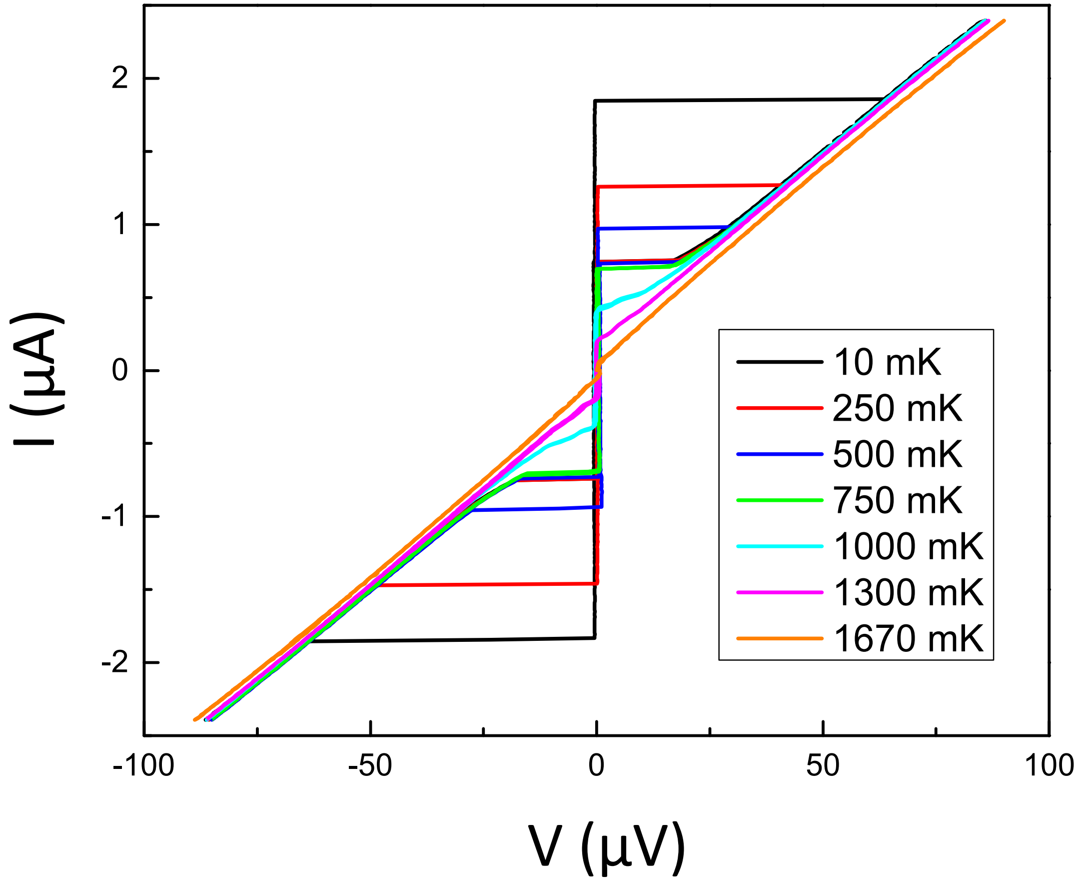

Kurter et al., PRB **90**, 014501 (2014).
Kurter et al., Nat. Commun. **6**, 7130 (2015).

Josephson Effect in TI

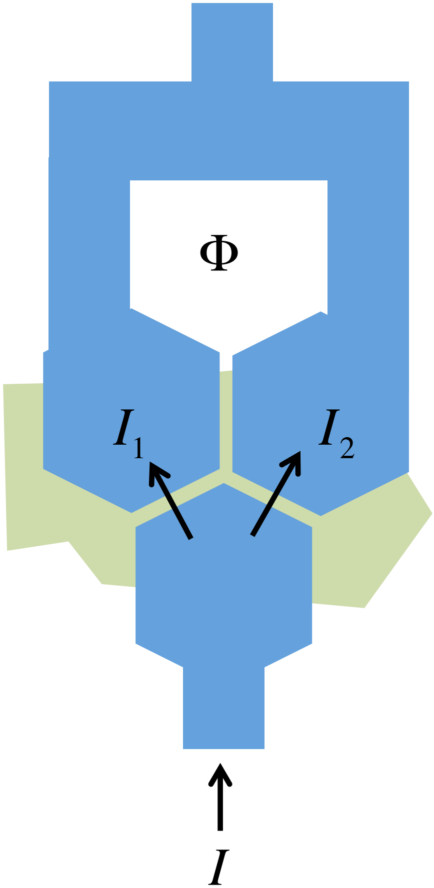

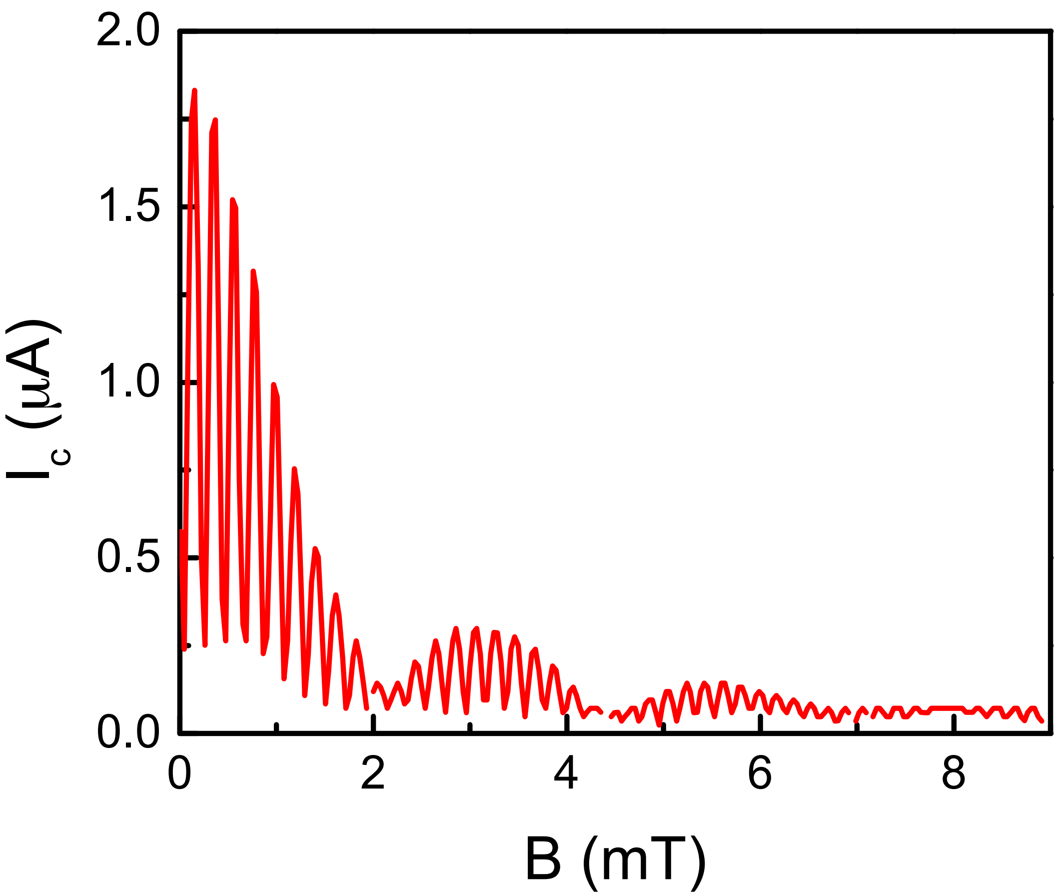

Kurter et al., PRB **90**, 014501 (2014).
Kurter et al., Nat. Commun. **6**, 7130 (2015).

Top Gate Dependence of Critical Current

Device 1 (9 nm thick)

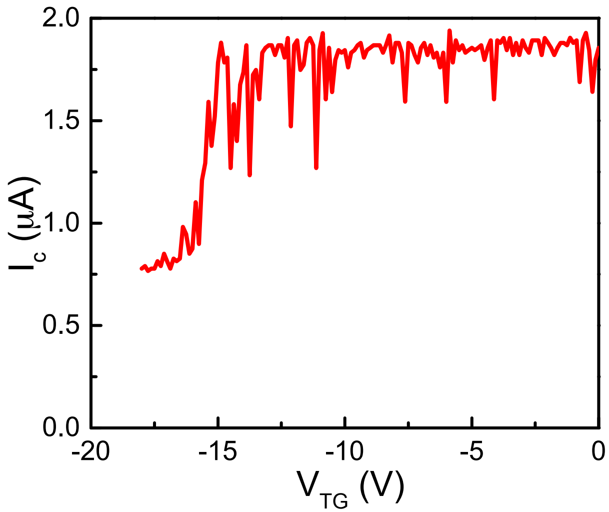

Device 2 (85 nm thick)

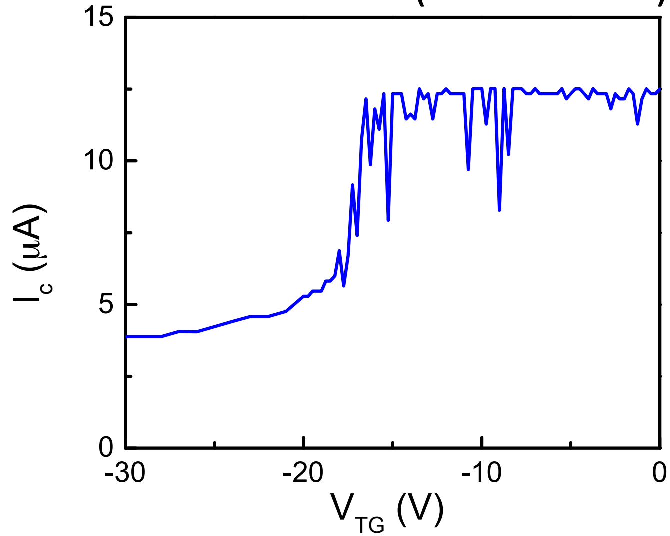

Device 3 (30 nm thick)

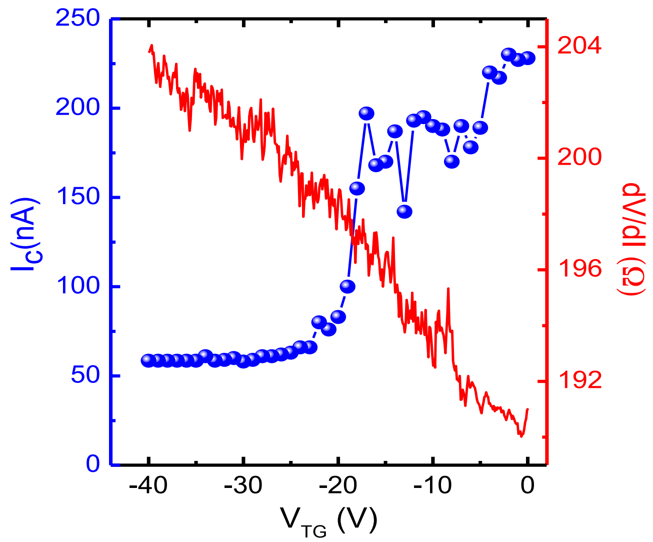

Sharp drop in critical current.
No such transition seen in normal state transport.

Kurter et al., PRB **90**, 014501 (2014).
Kurter et al., Nat. Commun. **6**, 7130 (2015).
Orlyanchik et al., arXiv: 1309.0163.

Majorana Fermion Induced Resonant Andreev Reflection

K. T. Law,[1,2] Patrick A. Lee,[2] and T. K. Ng[3]

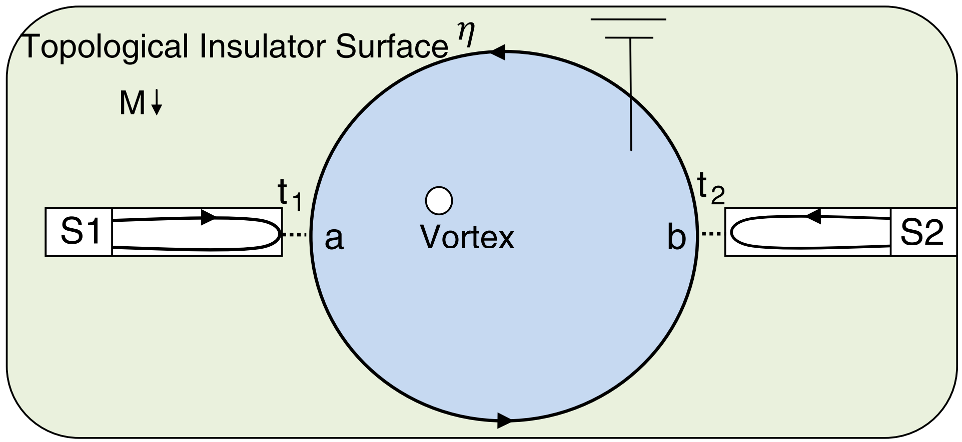

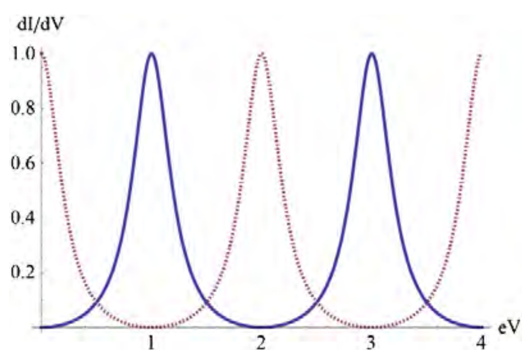

FIG. 3 (color online). dI/dV vs eV with $\tilde{t}_1^4 = 0.1$. eV is in units of $\pi\hbar v_m/L$ and dI/dV is in units of $\frac{2e^2}{h}$. Solid (dashed) line represents the case with even (odd) number of vortices in the superconductor.

Robust zero-energy peaks should emerge at odd number of vortices.

Majorana Interferometry

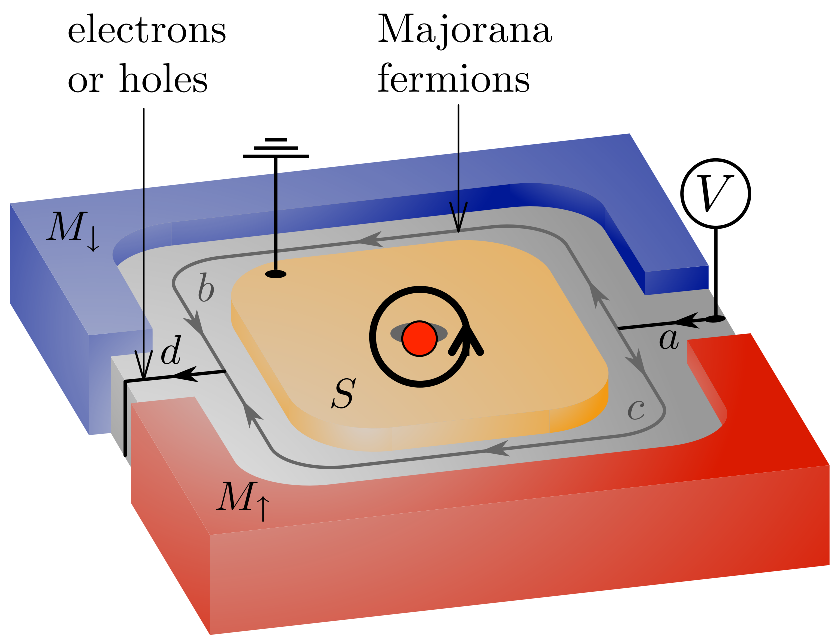

$$G(V)=\frac{2e^2}{h}|S_{he}(eV)|^2=\frac{2e^2}{h}\sin^2\!\left(\frac{n_v\pi}{2}+\frac{eV\delta L}{2\hbar v_m}\right).$$

Fu and Kane, Phys. Rev. Lett. **102**, 216403 (2009).
Akhmerov, Nilsson, and Beenakker, Phys. Rev Lett. **102**, 216404 (2009).

Quantum Interference in TIs

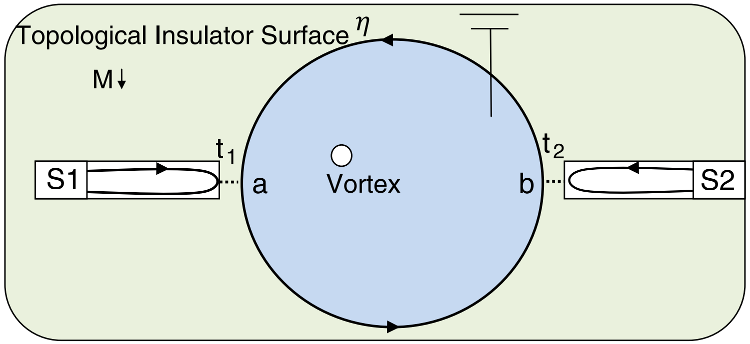

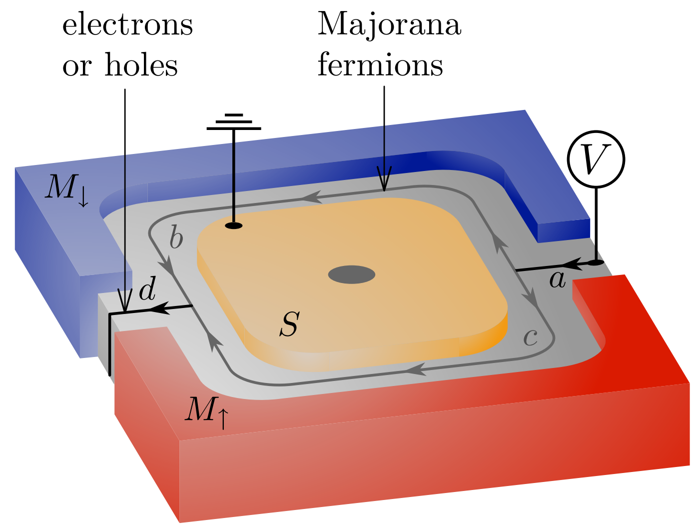

- Can we observe Fabry-Perot resonances in topological insulators?
- How do such resonances interact with…
  - Superconductivity?
  - Top and back gating?
  - Magnetic fields?

Andreev Spectroscopy Devices

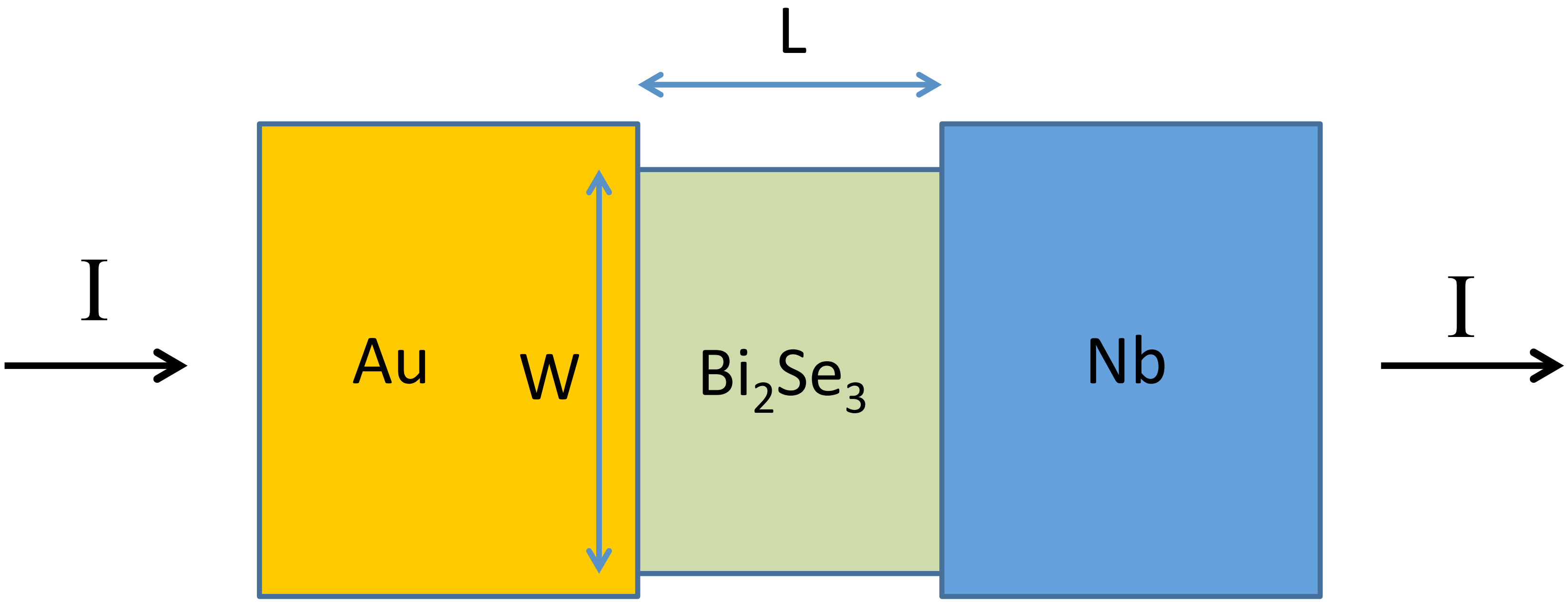

L = 100-400 nm

W = 250-500 nm

Bi_2Se_3 thickness = 10-20 nm

Andreev Spectroscopy Devices

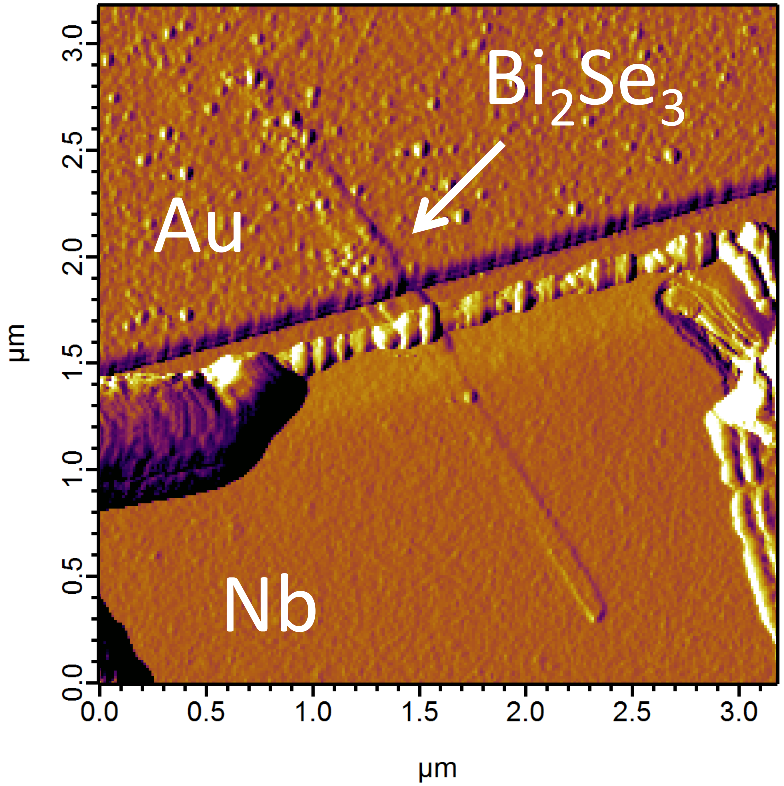

Back gated sample

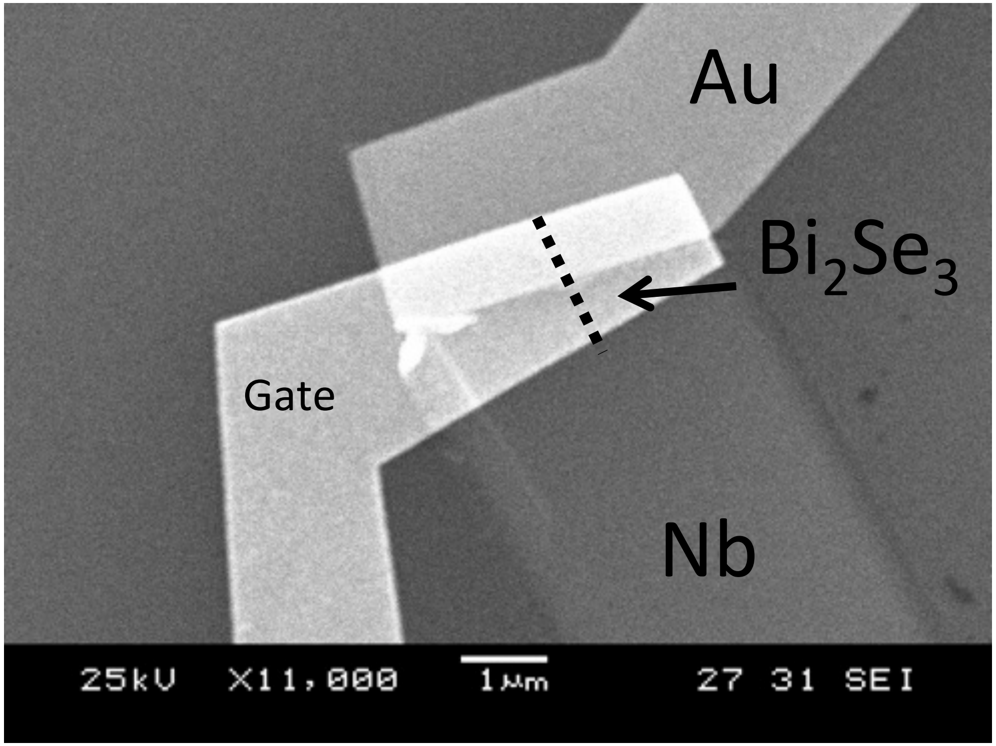

Sample with top gate

Transport at Zero Field

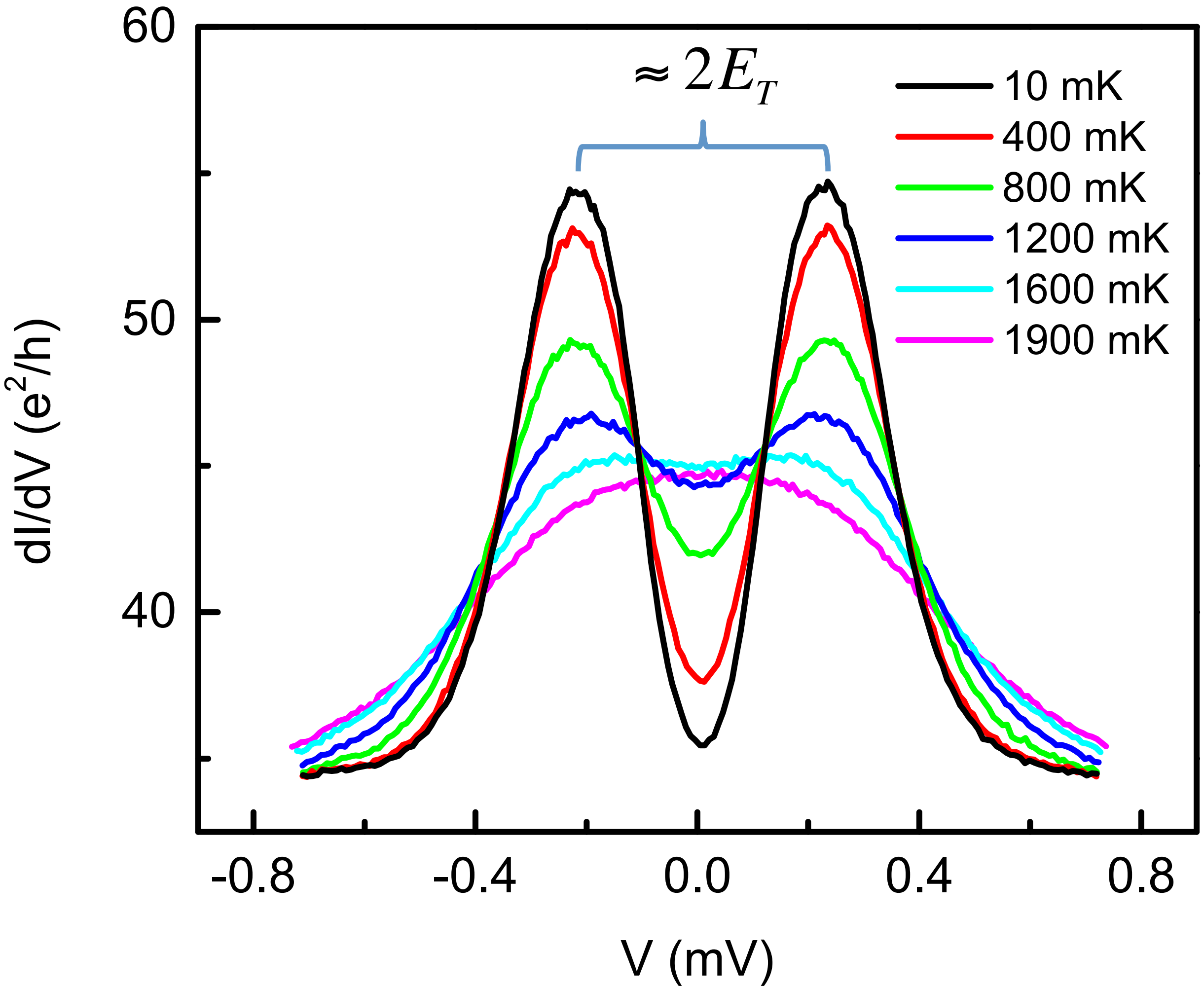

$$E_T = \frac{\hbar D}{L^2},$$

$$D = \tfrac{1}{2} v_F l \approx 0.0025\, m^2/s$$

For L = 100 nm:

$$E_T = 160\ \mu V$$

Re-entrant resistance effect due to competition between Andreev reflection and proximity-induced energy gap.

Artemenko et al., Solid State Comm. **30**, 771 (1979).

Gate Tuned Transport

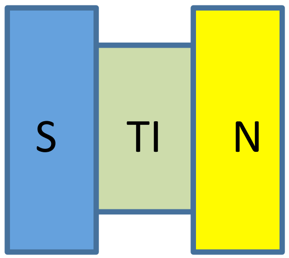

9 nm thick TI flake;
L = 230 nm

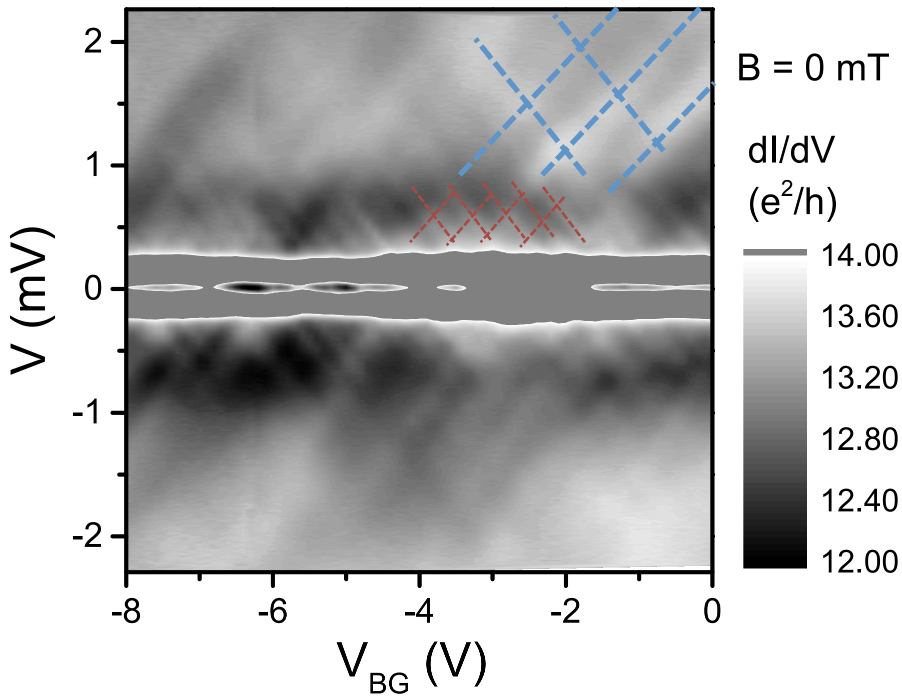

Fabry-Perot Oscillations

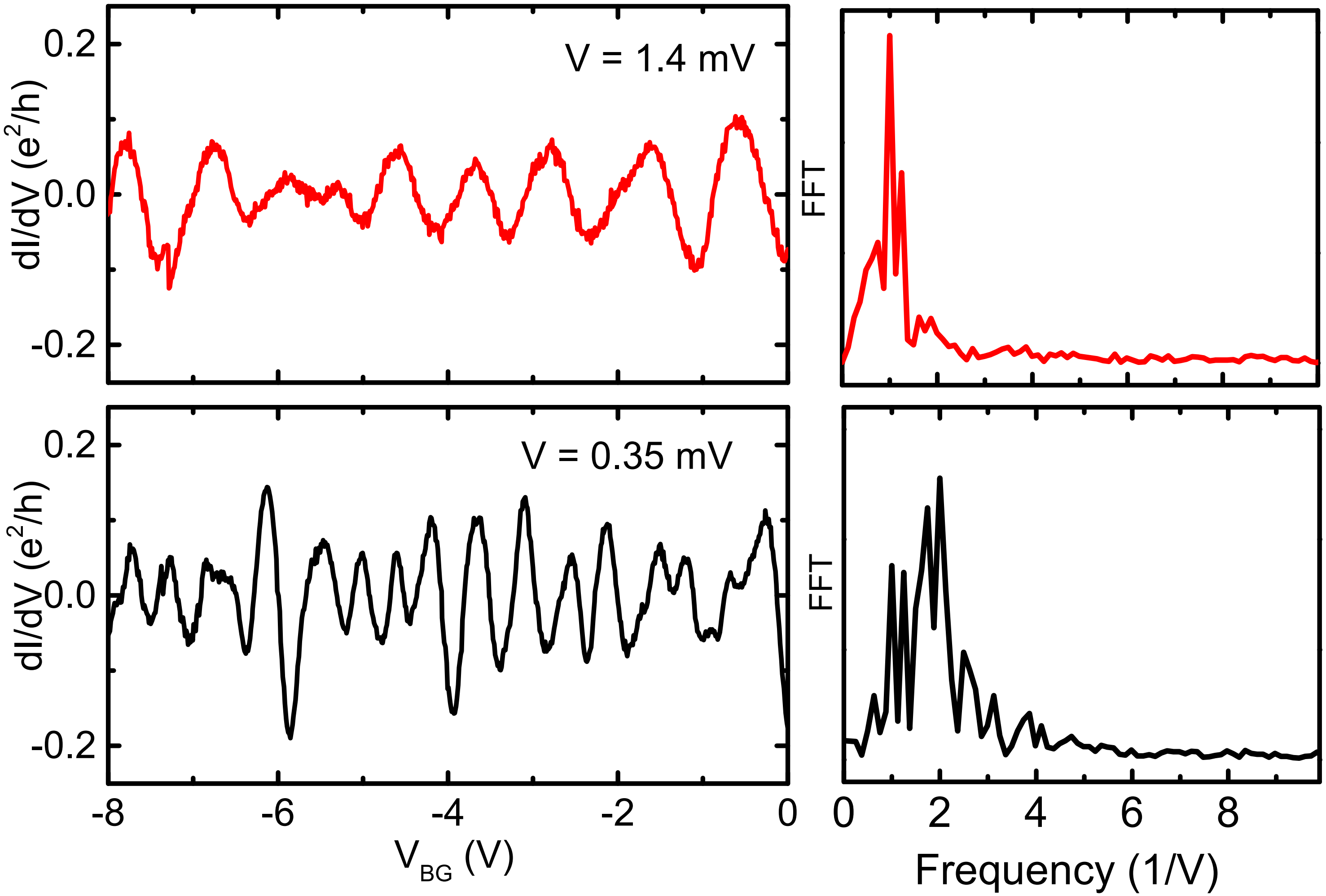

Low bias oscillations with period ΔV_{BG} = 0.5 V.

High bias oscillations with period ΔV_{BG} = 1 V.

Fabry-Perot + Andreev

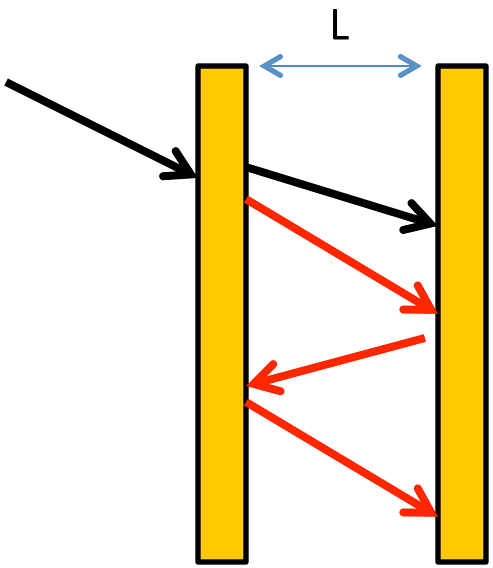

Path length difference between black and red: 2 L
Resonance :

$$2Lk_F = 2\pi n \longrightarrow \Delta E_F = \frac{hv_F}{2L}$$

(observed: 0.8 mV)
(expected: 3.8 mV)

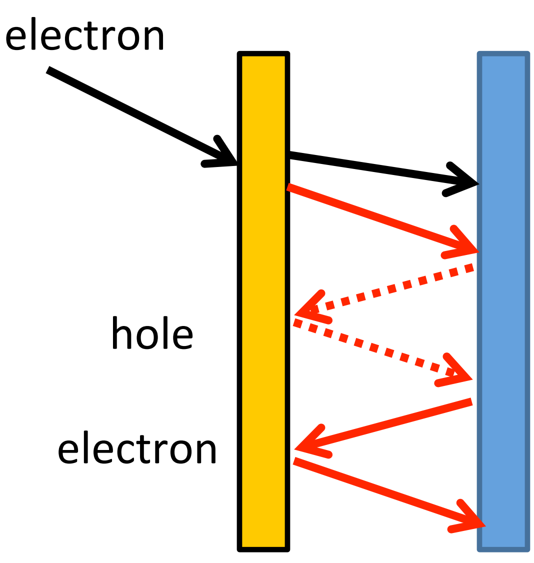

Path length difference between black and red: 4 L

$$\Delta E_F = \frac{hv_F}{4L}$$

De Gennes and Saint-James, Phys. Lett. 4, 151 (1963).
Rowell and McMillan, Phys. Rev Lett. 16, 453 (1966).
Finck et al., Phys. Rev. X 4, 041022 (2014).

Complications

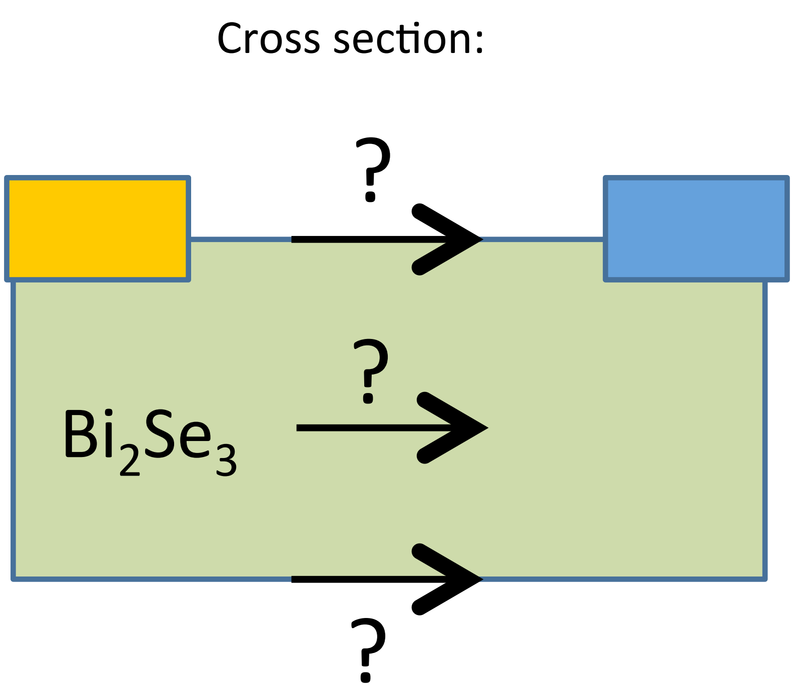

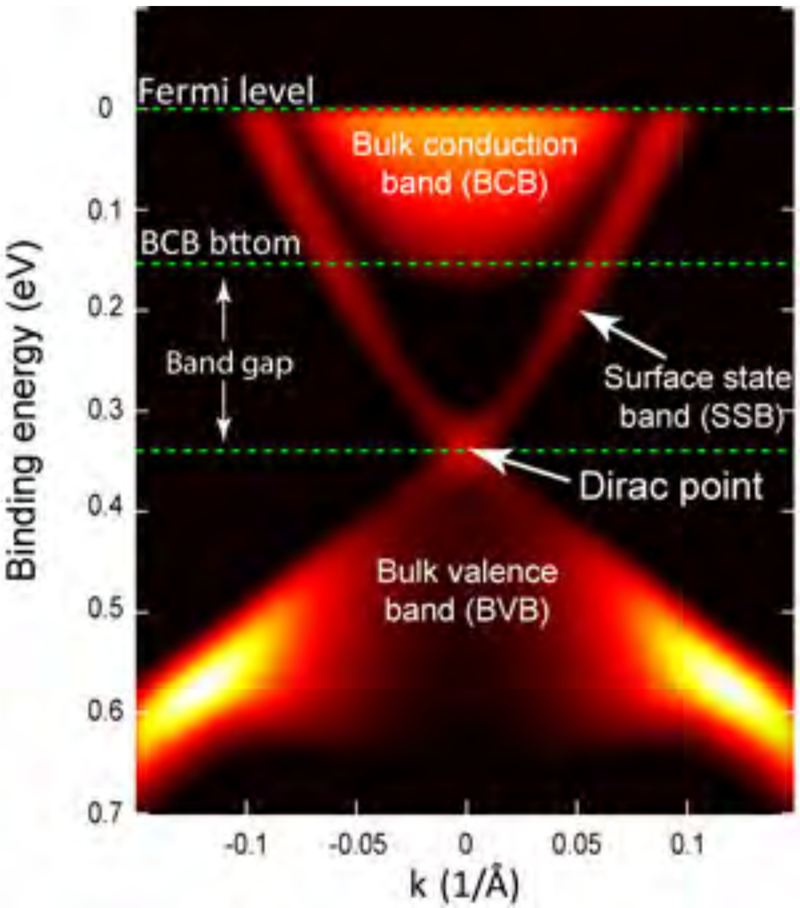

Various conductance channels are present.

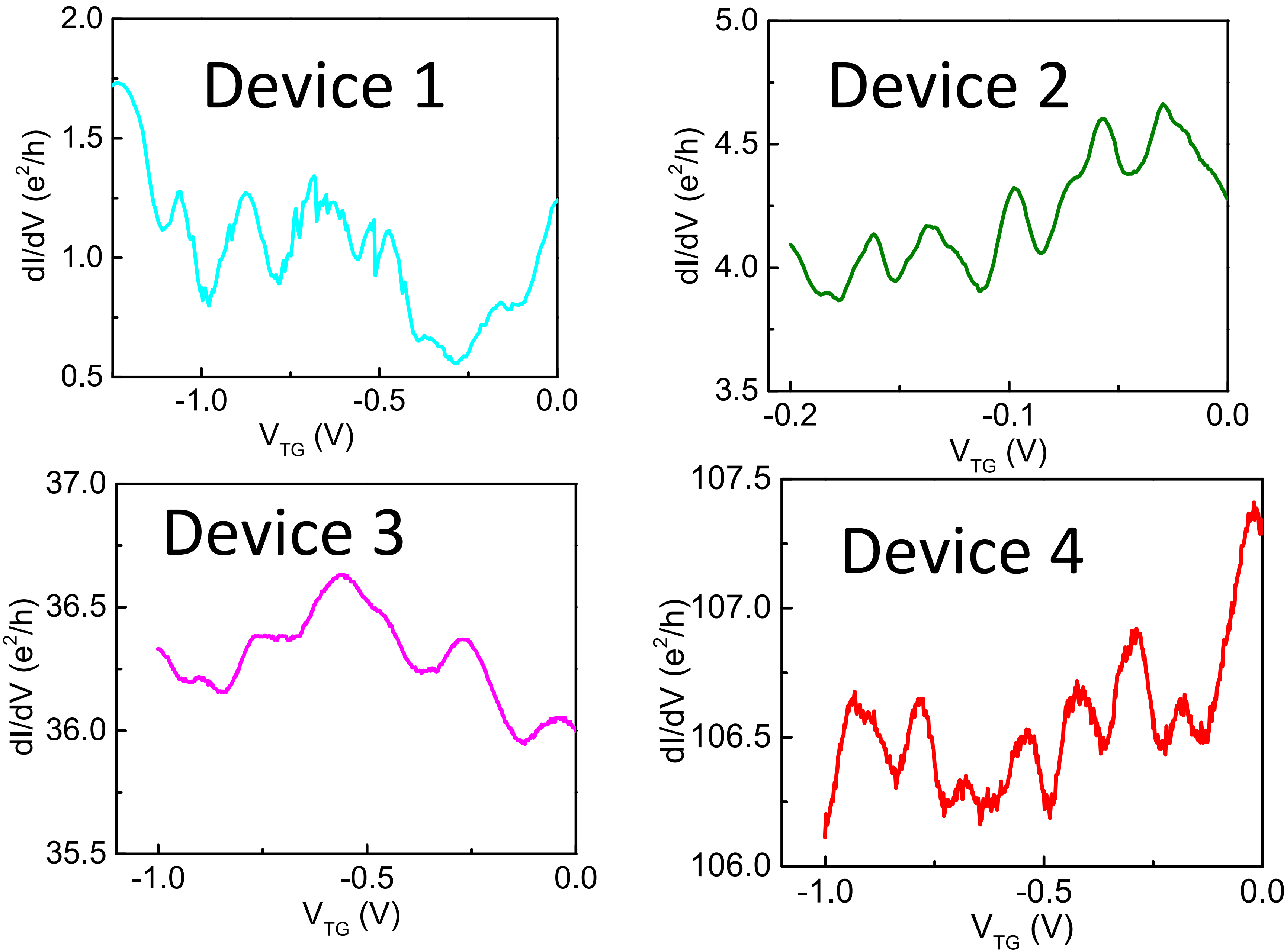

Amplitude of oscillations is roughly independent of bulk doping -> surface states?

Dual Gating of Resonances

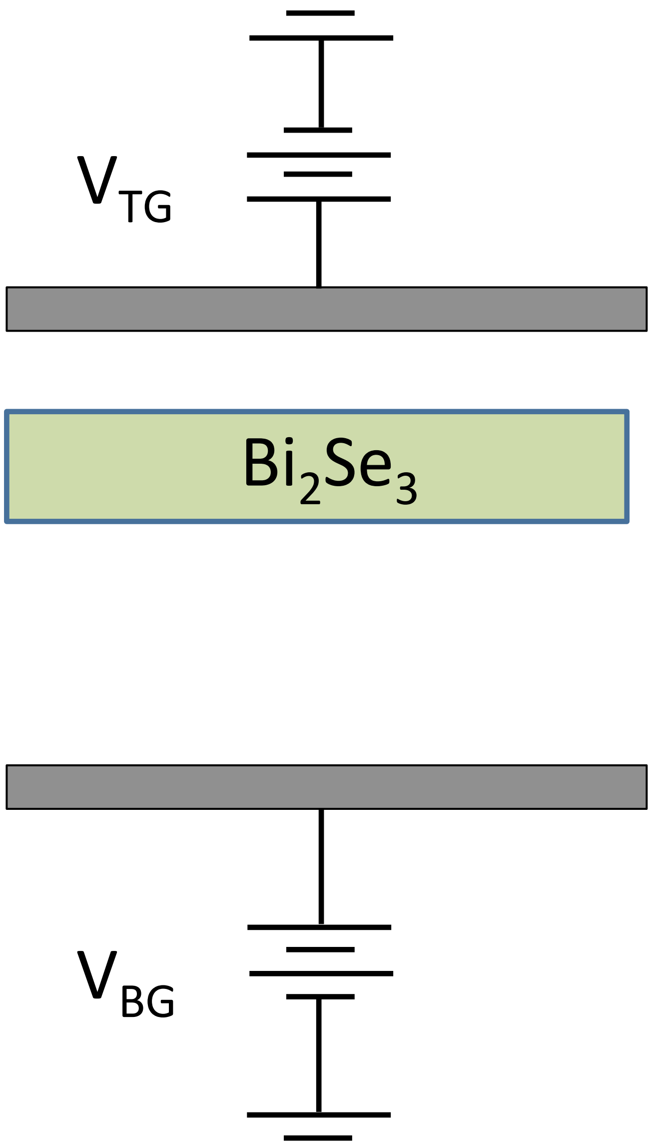

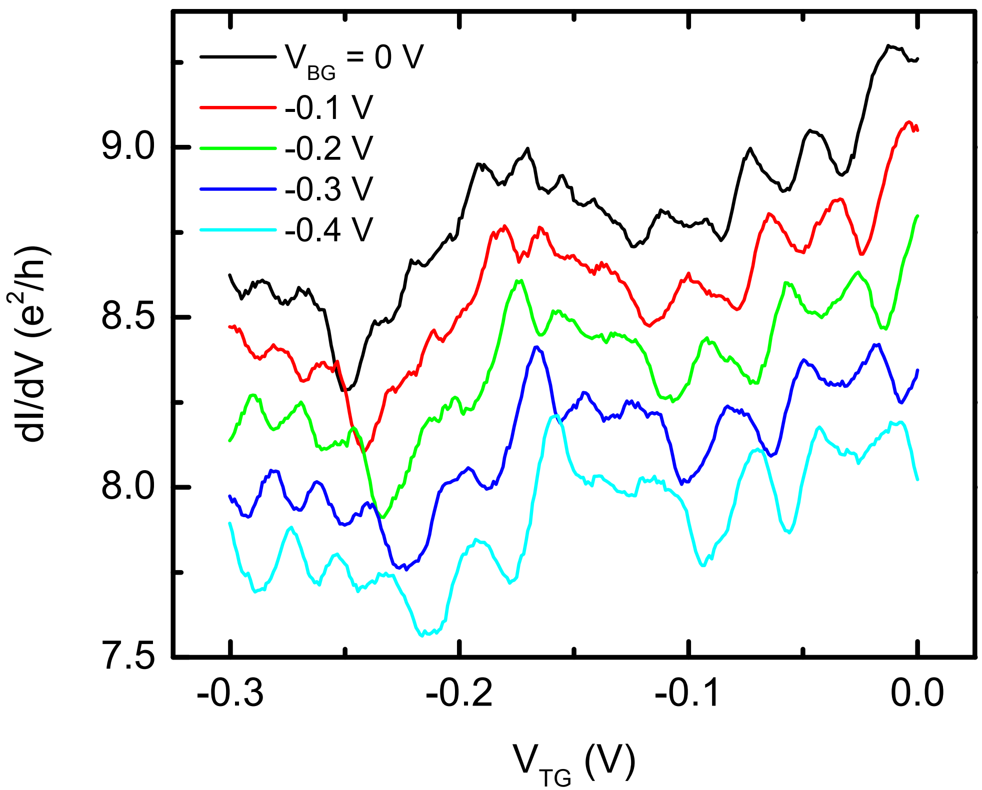

Dual Gating of Resonances

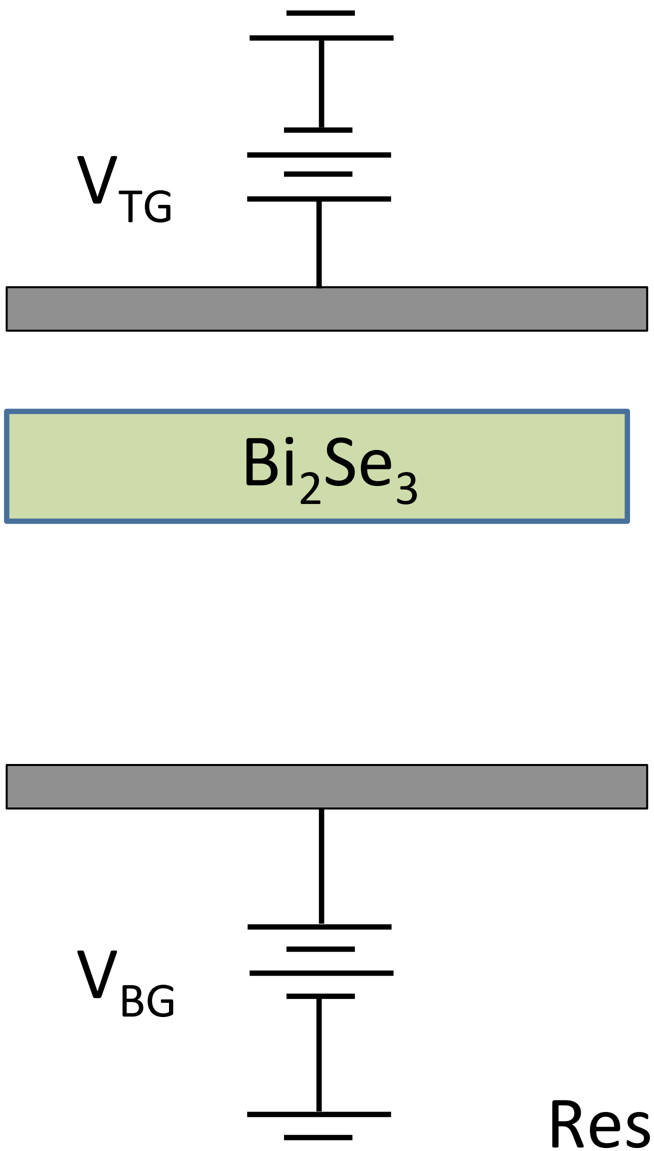

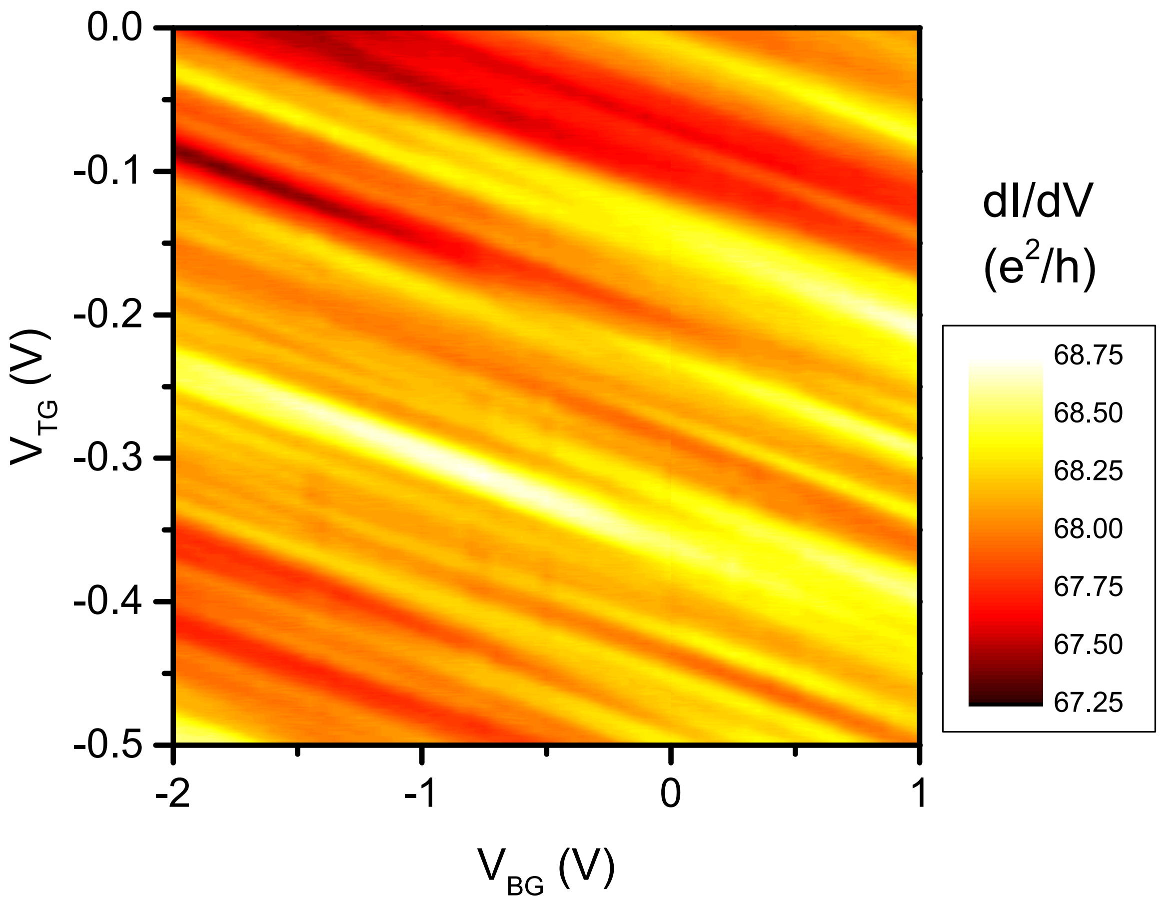

Resonances can be tuned by both gates.

Aharonov-Bohm Interferometer

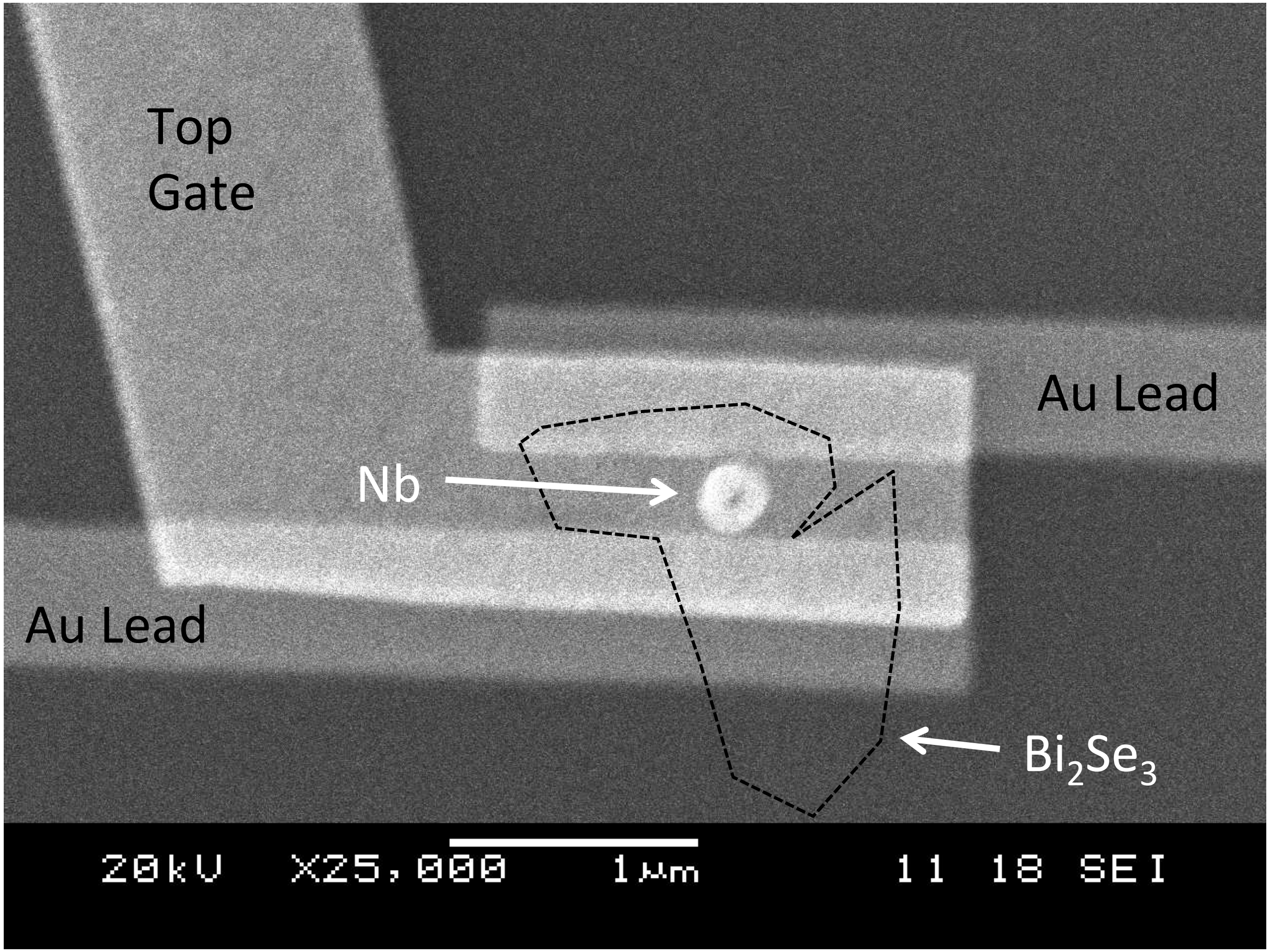

~200 nm wide niobium disk in the middle of a gold-TI-gold junction.

Magnetotransport

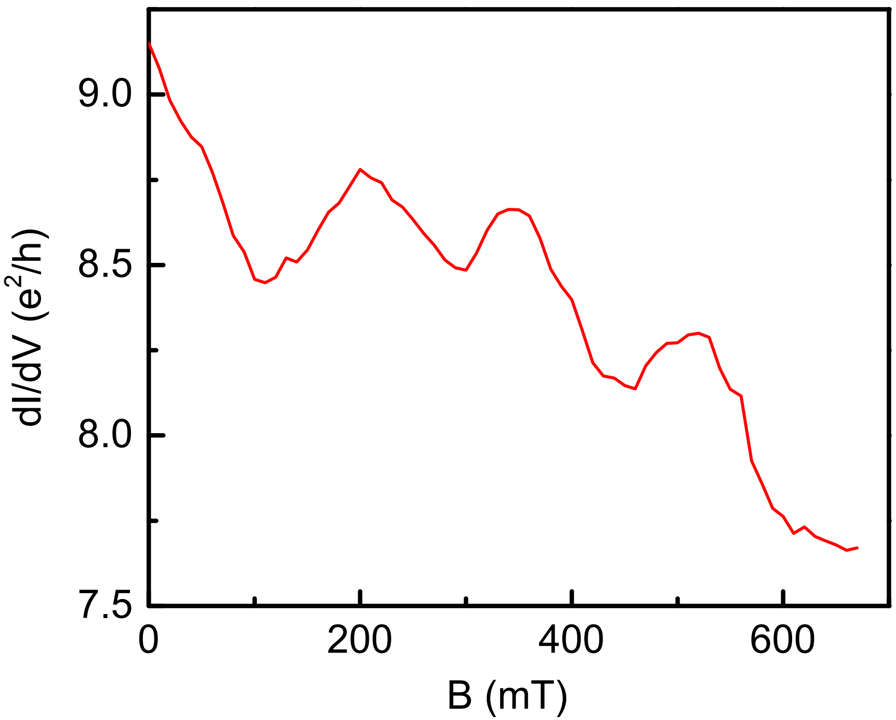

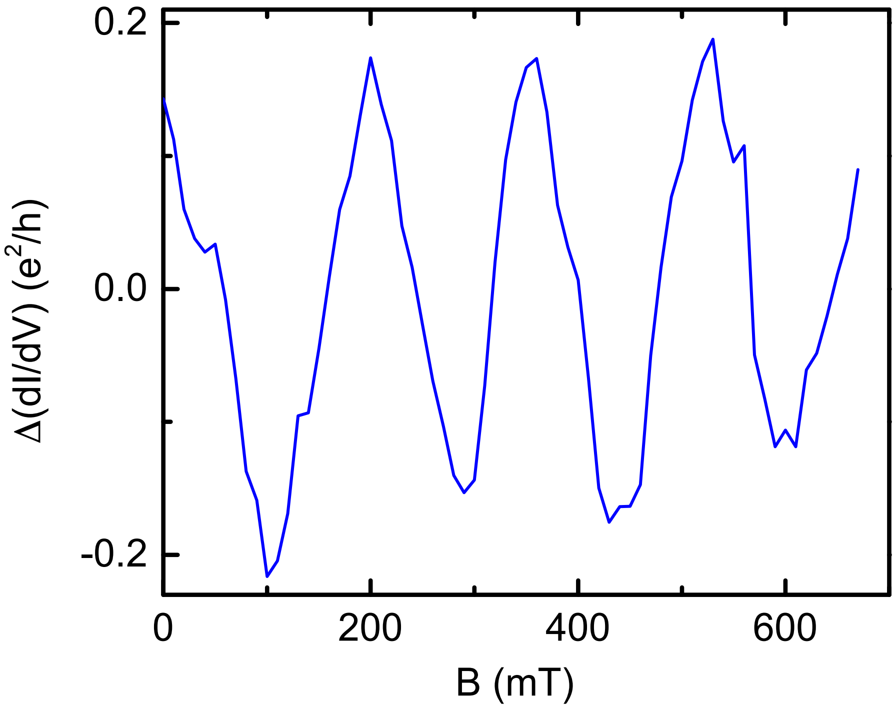

Conductance oscillations with period of ~200 mT.

Aharonov-Bohm Oscillations

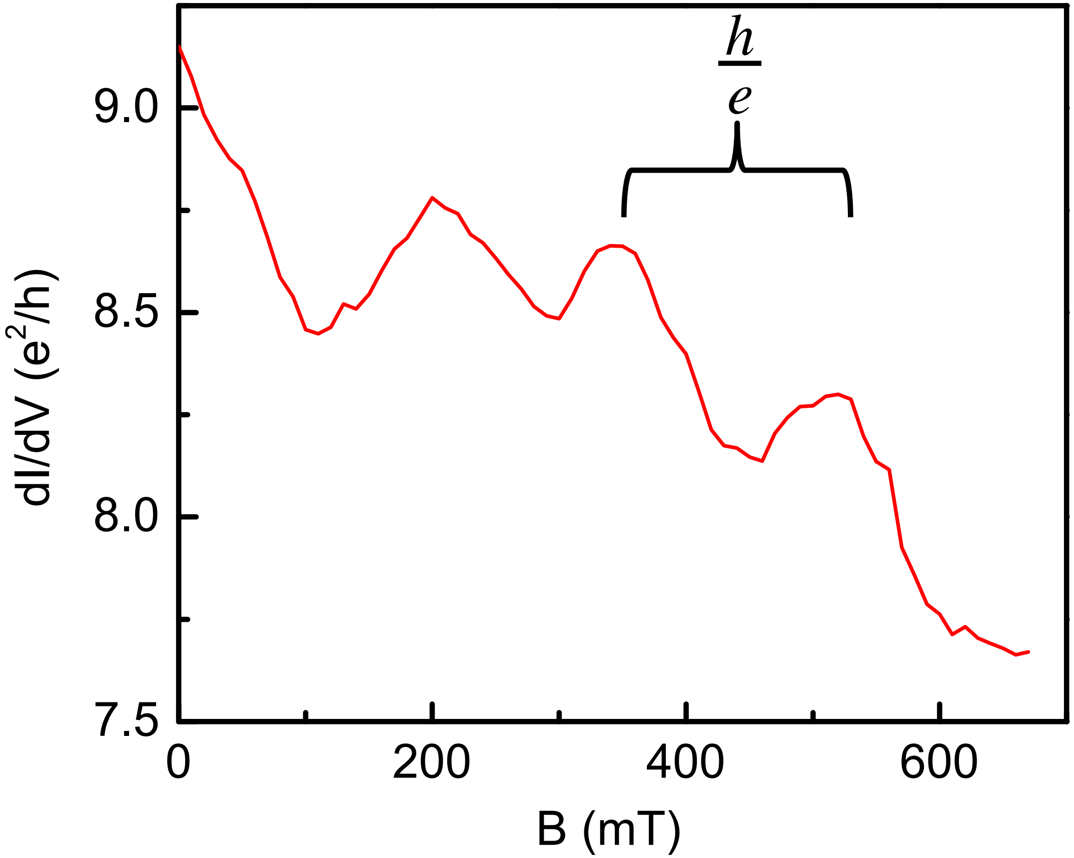

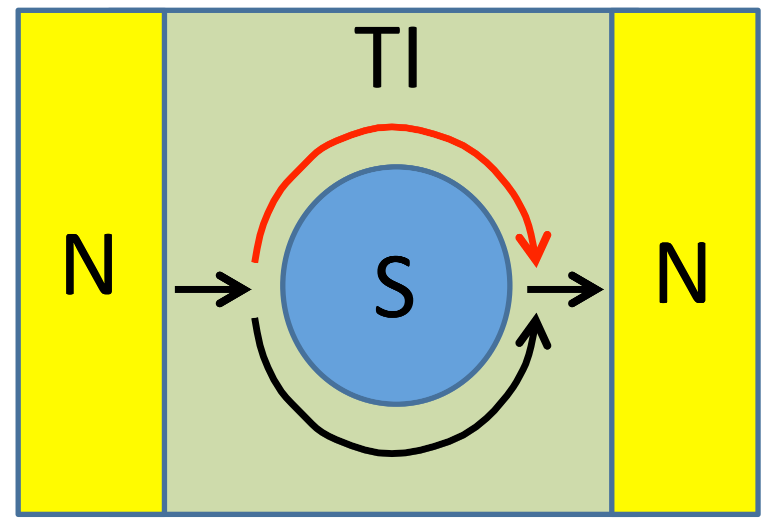

Oscillation period corresponds to area of superconductor.

Gate Sweeps at High Field

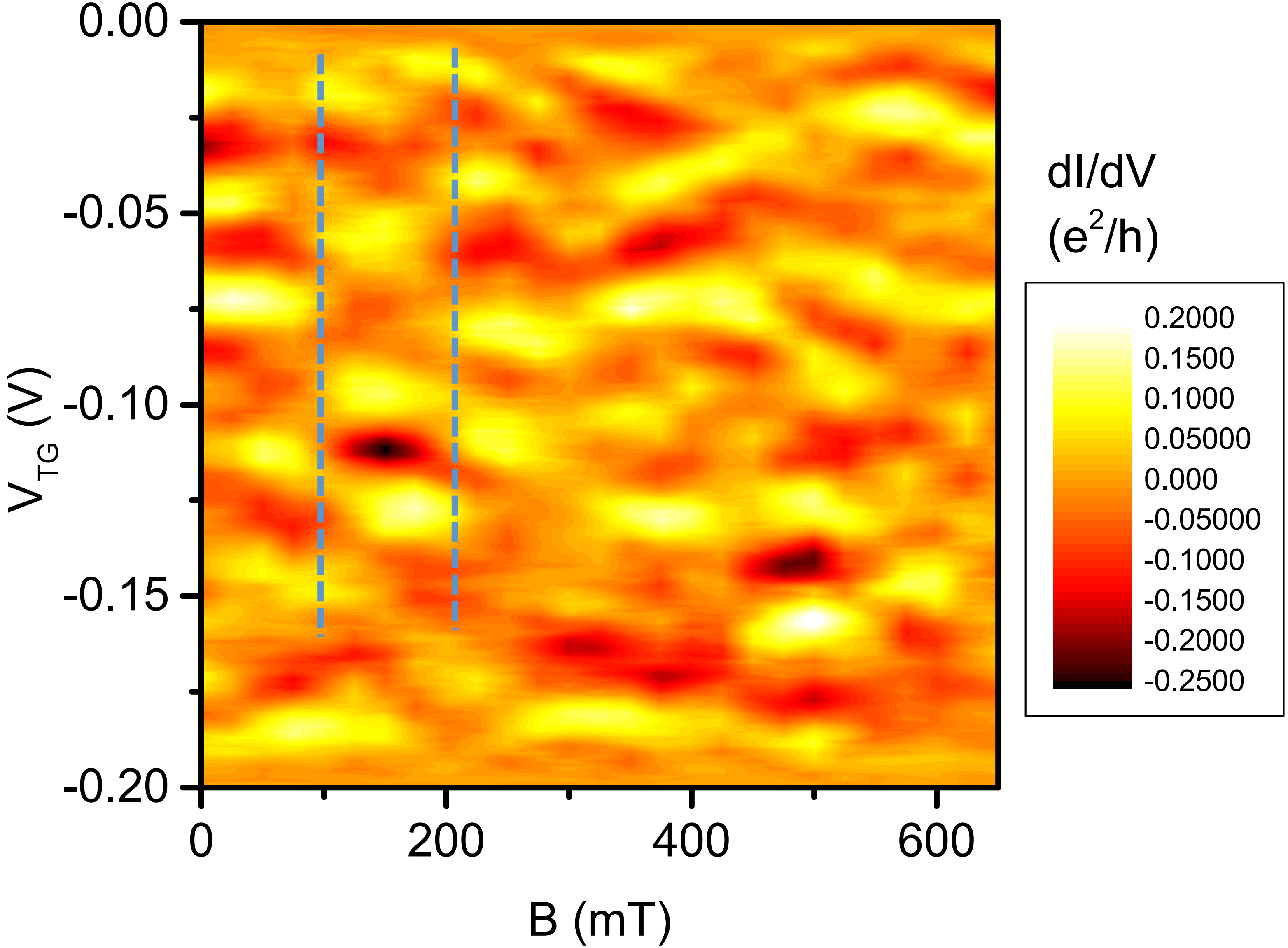

Signs of checkerboard pattern.

Oscillations in Larger Device

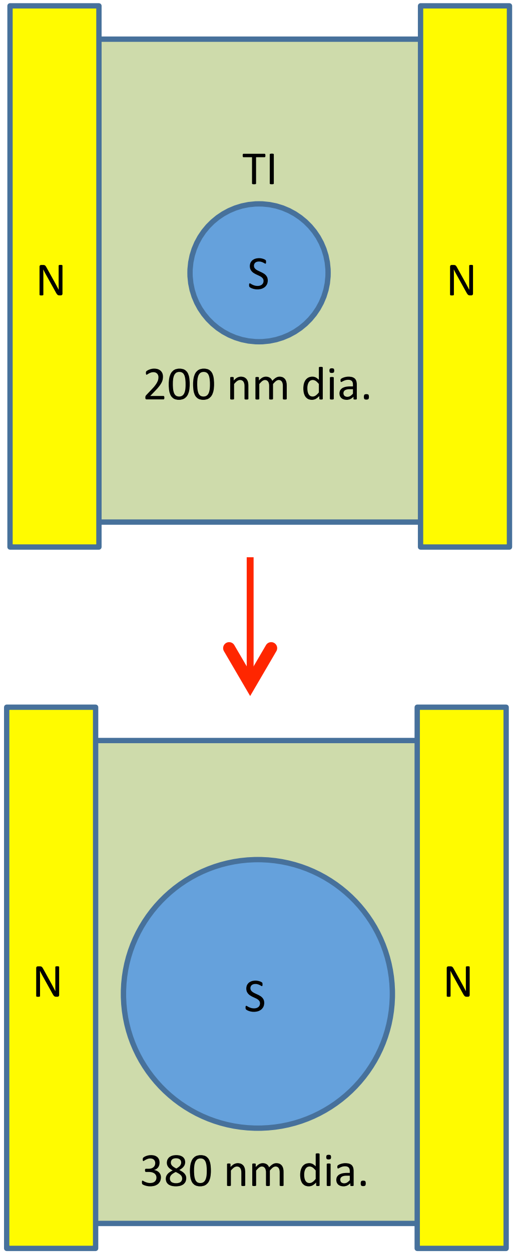

380 nm diameter dot:

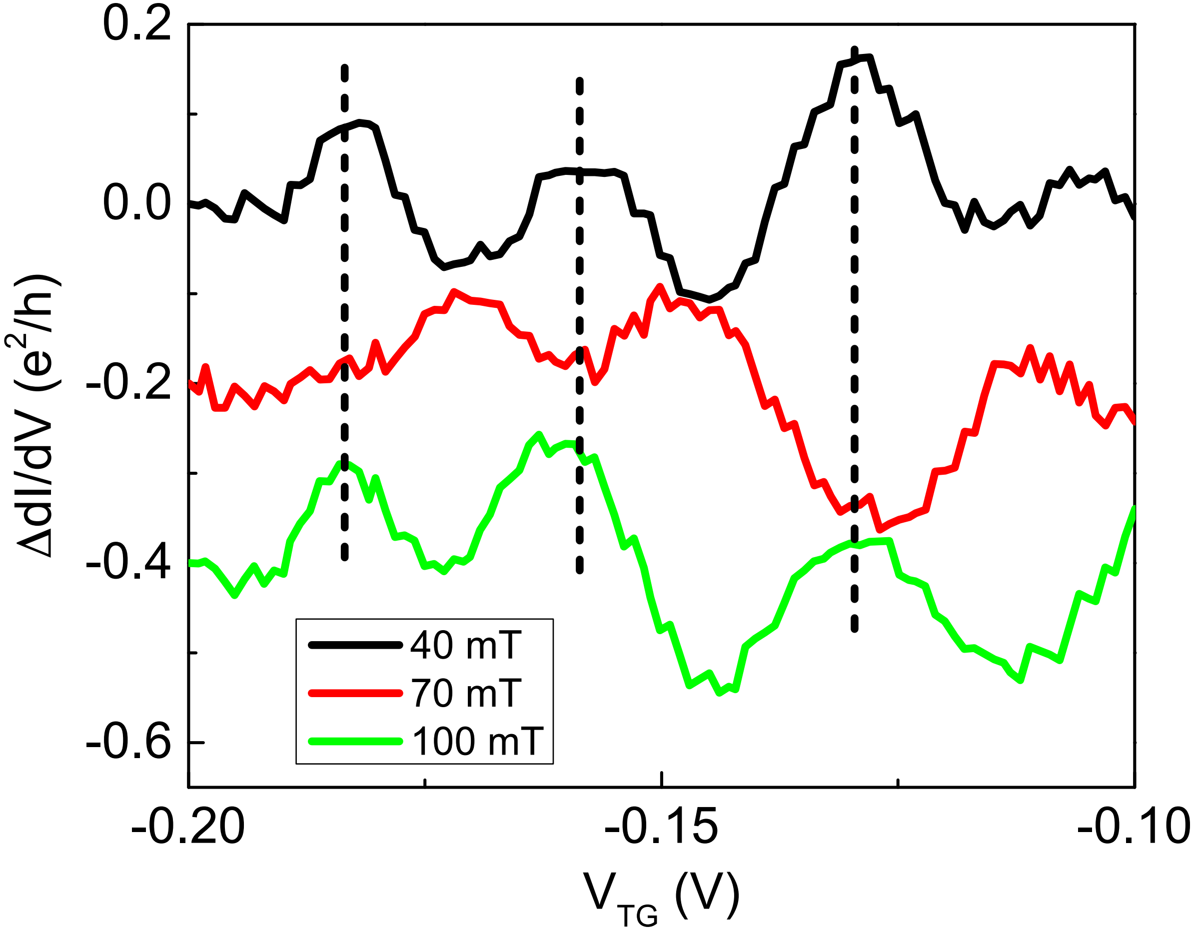

Field periodicity scales with Nb area.

Off-Center Niobium Disk

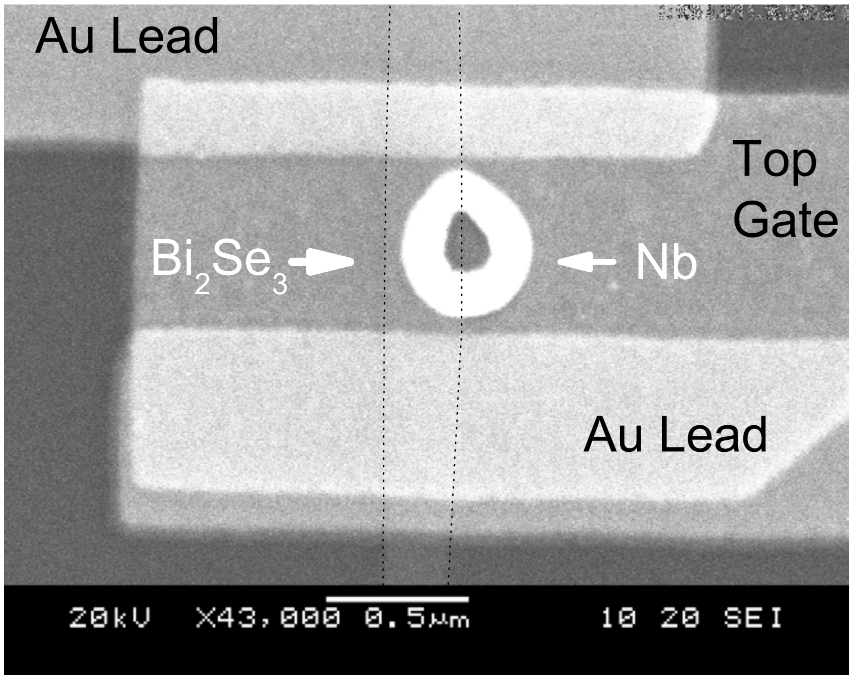

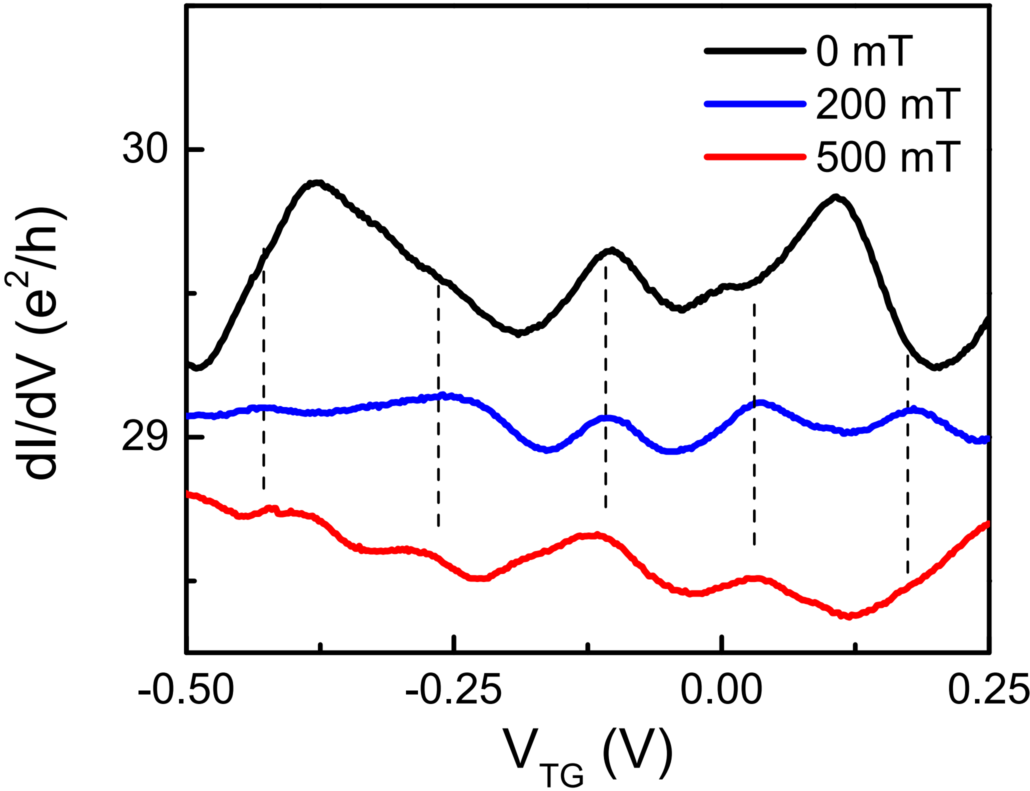

No phase shift observed.

Off-Center Niobium Disk

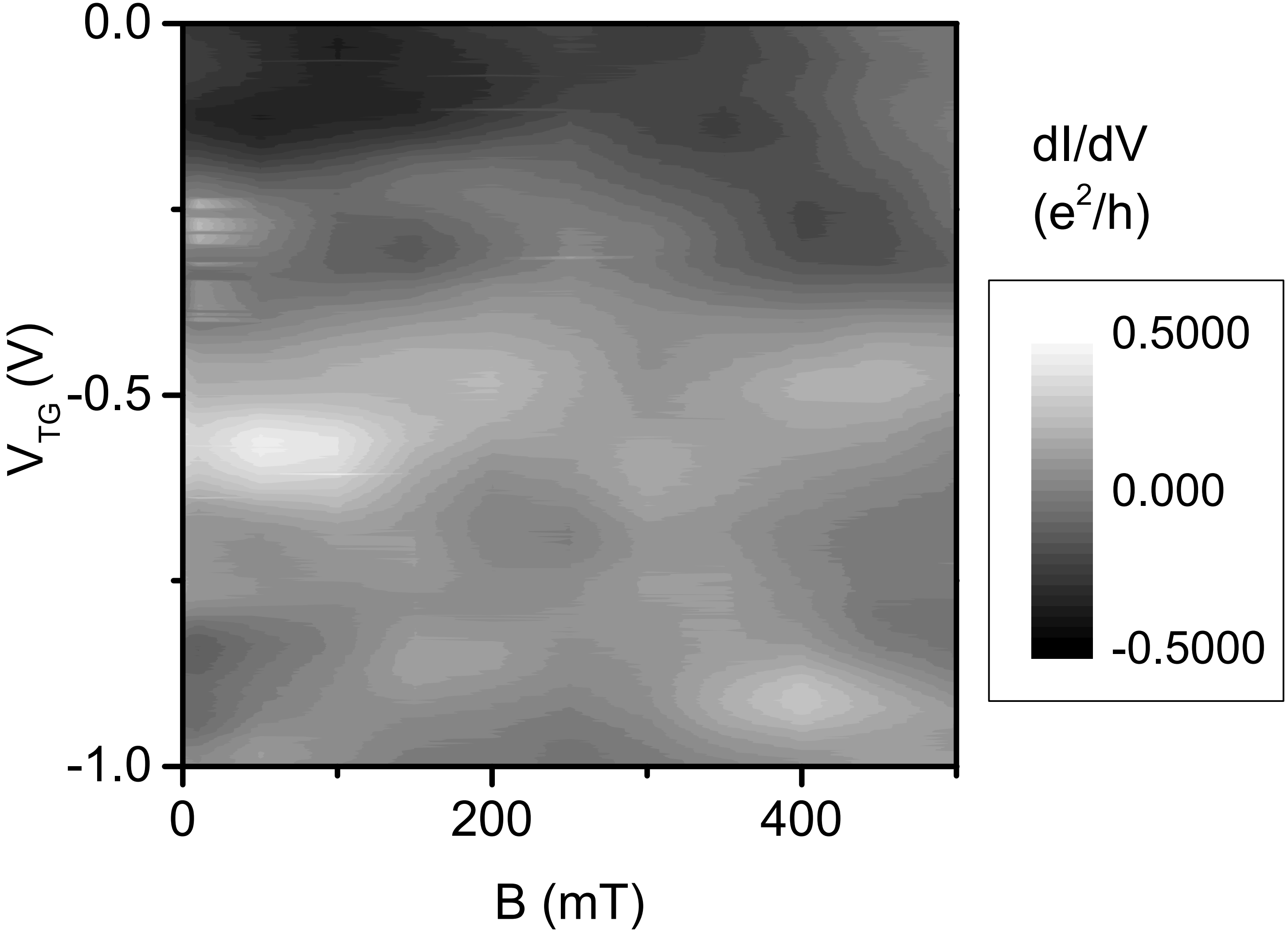

Disk Extending Entire Width

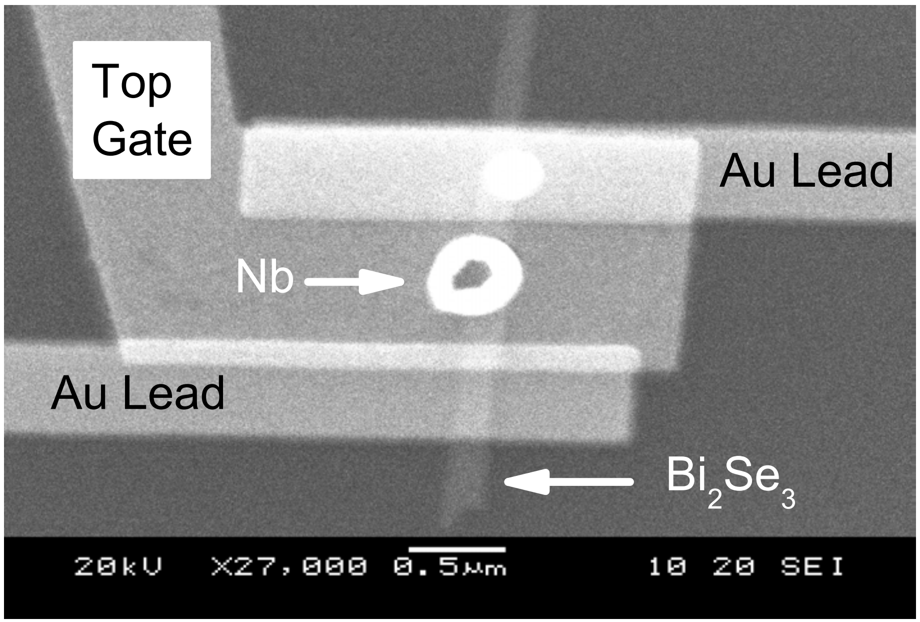

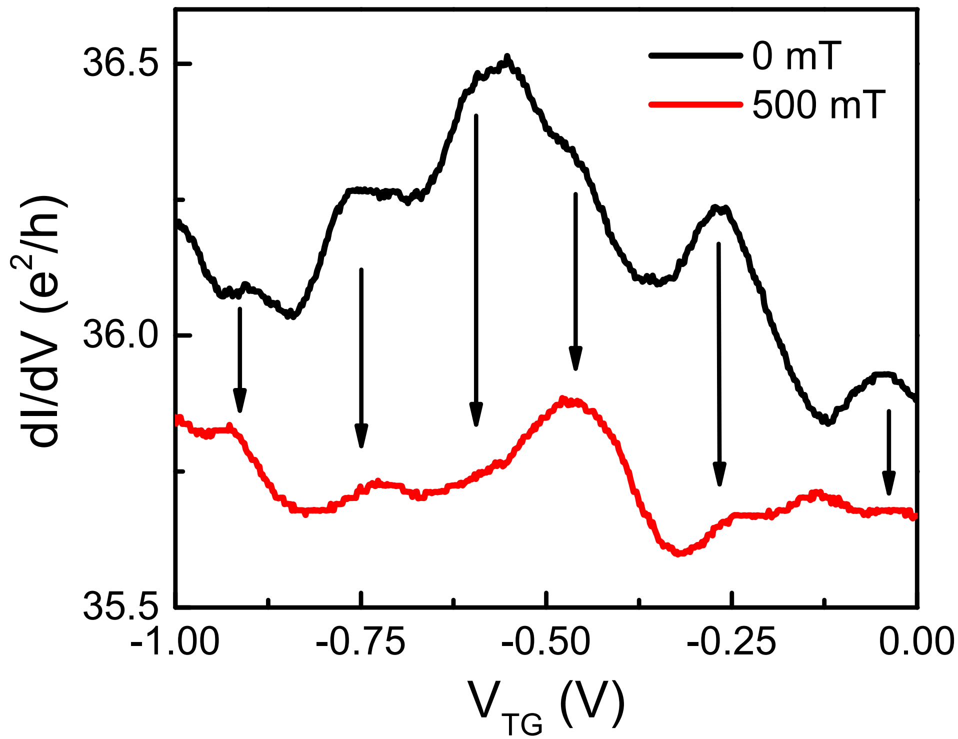

No phase shift observed without multiply-connected geometry.

Phase Shift from Majoranas?

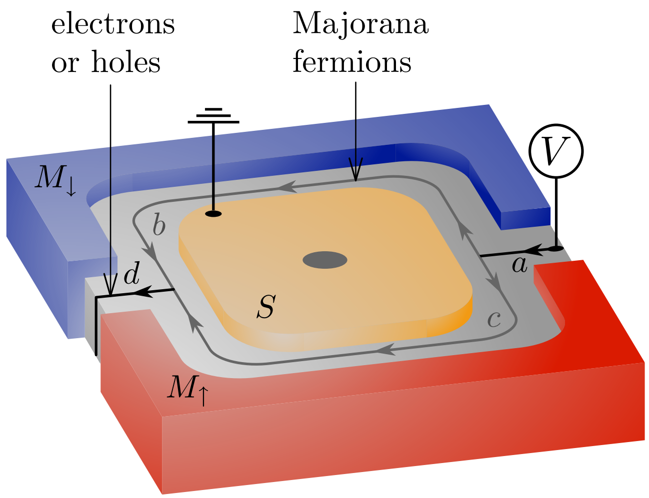

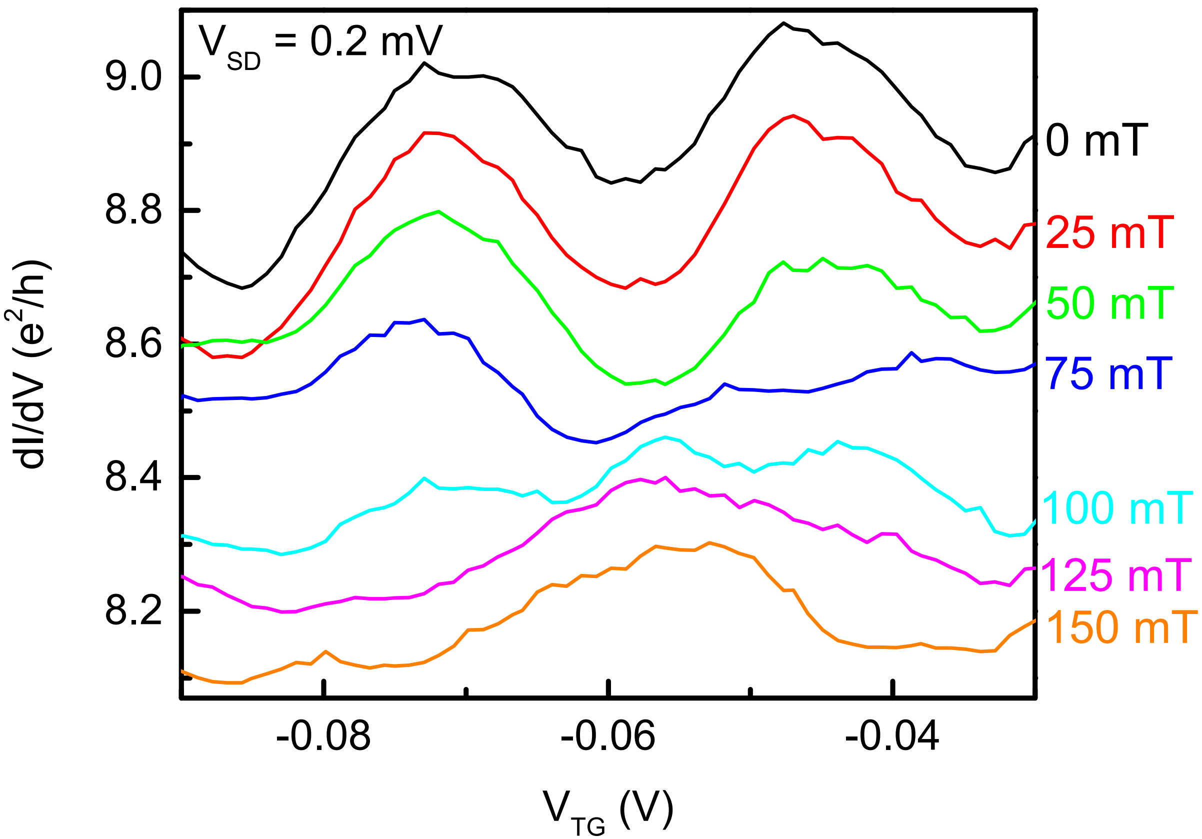

Phase shift is rapid yet smooth.

Conclusions

Realization of Fabry-Perot interferometers in topological insulators.

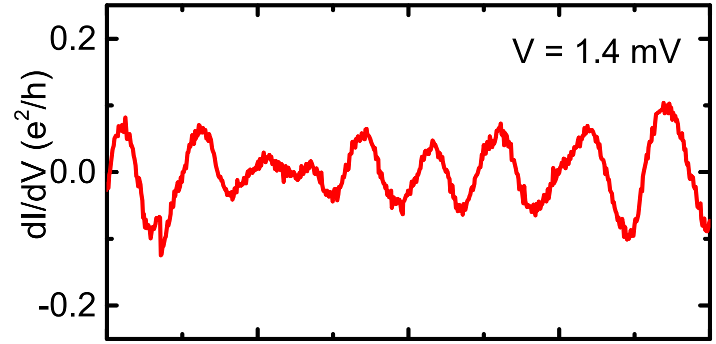

Observation of interplay between phase coherence and Andreev reflection.

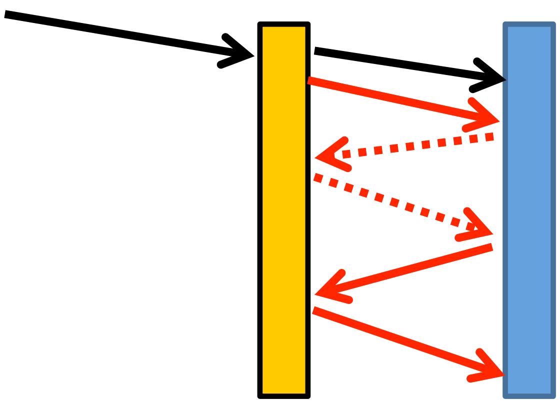

Anomalous phase shift from Aharonov-Bohm effect, suggesting edge states.